

1 **Early mannitol-triggered changes in the Arabidopsis leaf (phospho)proteome**

2

3 Natalia Nikonorova<sup>1,2,\*</sup>, Lisa Van den Broeck<sup>1,2,\*</sup>, Shanshuo Zhu<sup>1,2,3,4</sup>, Brigitte van de  
4 Cotte<sup>1,2</sup>, Marieke Dubois<sup>1,2,\$</sup>, Kris Gevaert<sup>1,2,3,4</sup>, Dirk Inzé<sup>1,2</sup>, and Ive De Smet<sup>1,2,#</sup>

5

6 <sup>1</sup> Ghent University, Department of Plant Biotechnology and Bioinformatics, 9052 Ghent,  
7 Belgium

8 <sup>2</sup> VIB Center for Plant Systems Biology, 9052 Ghent, Belgium

9 <sup>3</sup> Ghent University, Department of Biochemistry, 9052 Ghent, Belgium

10 <sup>4</sup> VIB Center for Medical Biotechnology, 9052 Ghent, Belgium

11

12 <sup>\$</sup>Present address: Institut de Biologie Moléculaire des Plantes, CNRS, 67084 Strasbourg,  
13 France

14

15 <sup>\*</sup>Equal contribution

16

17 <sup>#</sup>CORRESPONDING AUTHOR: Ive De Smet, VIB-UGent Center for Plant Systems  
18 Biology, Technologiepark 927, 9052 Gent, Belgium, Tel: +3293313930, E-mail:  
19 [ivsme@psb.vib-ugent.be](mailto:ivsme@psb.vib-ugent.be)

20

21 RUNNING TITLE: Early mannitol-triggered changes in Arabidopsis leaf phosphoproteome

22

23

24 **ABSTRACT**

25

26 Drought is one of the most detrimental environmental stresses to which plants are exposed.  
27 Especially mild drought is relevant to agriculture and significantly affects plant growth and  
28 development. In plant research, mannitol is often used to mimic drought stress and study the  
29 underlying responses. In growing leaf tissue of plants exposed to mannitol-induced stress, a  
30 highly-interconnected gene regulatory network is induced. However, early signaling and  
31 associated protein phosphorylation events that likely precede part of these transcriptional  
32 changes are largely unknown. Here, we performed a full proteome and phosphoproteome  
33 analysis on growing leaf tissue of *Arabidopsis* plants exposed to mild mannitol-induced stress  
34 and captured the fast (within the first half hour) events associated with this stress. Based on  
35 this in-depth data analysis, 167 and 172 differentially regulated proteins and phosphorylated  
36 sites were found back, respectively. Additionally, we identified H(+)-ATPASE 2 (AHA2)  
37 and CYSTEINE-RICH REPEAT SECRETORY PROTEIN 38 (CRRSP38) as novel  
38 regulators of shoot growth under osmotic stress.

39

40 **HIGHLIGHT**

41 We captured early changes in the *Arabidopsis* leaf proteome and phosphoproteome upon mild  
42 mannitol stress and identified AHA2 and CRRSP38 as novel regulators of shoot growth  
43 under osmotic stress.

44

45 **KEYWORDS**

46 Signalling, Phosphoproteome, Mild osmotic stress, *Arabidopsis thaliana*, AHA2, CRRSP38

47

48

## 49 INTRODUCTION

50

51 Plants are exposed to a range of disadvantageous environmental conditions, which has led to  
52 the development of various molecular coping mechanisms (Wang *et al.*, 2017a; Berens *et al.*,  
53 2017; Demarsy *et al.*, 2017). Drought is one of the most detrimental environmental stresses to  
54 which plants are exposed (Boyer, 1982; Wang *et al.*, 2003). Plant growth and subsequently  
55 plant yield are drastically decreased as a result of drought. In a temperate climate, water  
56 scarcity rarely threatens the survival of the plant, but rather reduces the growth and yield of  
57 the crop. Undoubtedly, the underlying molecular mechanisms differ depending on how  
58 severe the water limitation is, as plant lines that are more tolerant to severe stress rarely  
59 perform better under mild stress (Skirycz *et al.*, 2011c). Because mild drought is more  
60 relevant to agriculture and significantly affects plant growth and development, studies on  
61 growth responses of plants exposed to mild drought are of increasing importance  
62 (Aguirrezabal *et al.*, 2006; Pereyra-Irujo *et al.*, 2008; Clauw *et al.*, 2015). Several studies  
63 have focussed on unravelling the transcriptomic changes associated with the drought  
64 response (Harb *et al.*, 2010; Clauw *et al.*, 2015, 2016; Bac-Molenaar *et al.*, 2016; Rasheed *et*  
65 *al.*, 2016; Dubois *et al.*, 2017; Verslues, 2017) and a few studies even addressed drought  
66 response on a proteome or phosphoproteome level (Singh and Jwa, 2013; Katam *et al.*, 2016;  
67 Vu *et al.*, 2016).

68 Capturing the early response upon drought, a condition that builds up gradually, is not  
69 straightforward. Because drought is associated with osmotic stress, *in vitro* alternatives, such  
70 as mannitol, sorbitol or polyethylene glycol (PEG), are used to study the molecular events  
71 associated with this stress condition (Verslues *et al.*, 2006a). By transferring plants at a  
72 desired time point during development to an osmotic compound or by adding such a  
73 compound to liquid cultures, the very early signalling mechanisms associated with osmotic

74 stress can be revealed. Low concentrations of mannitol (25 mM) induce mild stress,  
75 triggering a decrease in Arabidopsis rosette size of approximately 50% without affecting the  
76 plant's development or survival (Claeys *et al.*, 2014). Mannitol can therefore be used as a  
77 growth-repressive compound and has been shown to be ideal for studying growth-regulating  
78 events (Skiryicz *et al.*, 2011c; Van den Broeck *et al.*, 2017).

79 The osmotic stress responses in young growing leaves are very different from those in  
80 mature leaves. For example, in young leaves, mild stress induces the rapid accumulation of  
81 the ethylene precursor ACC (1-aminocyclopropane-1-carboxylate) and presumably also  
82 ethylene itself, instead of the classic drought-related hormone abscisic acid (ABA) (Skiryicz  
83 *et al.*, 2011a). Unravelling the growth regulation upon stress is thus preferably studied in  
84 growing tissue instead of mature leaves or whole seedlings, as growing tissues are more  
85 subdued by growth inhibitory mechanisms. In growing leaf tissue exposed to mannitol-  
86 induced stress, a highly-interconnected gene regulatory network (GRN) is induced. The  
87 transcription factors that are part of this network regulate each other's expression and have  
88 been shown to regulate leaf growth upon osmotic stress (Van den Broeck *et al.*, 2017). Some  
89 members of this GRN, such as ETHYLENE RESPONSE FACTOR 6 (ERF6), ERF9 and  
90 WRKY15, can activate the expression of *GIBBERELLIN2-OXIDASE6* (*GA2-OX6*), a gene  
91 encoding a gibberellin degradation enzyme (Rieu *et al.*, 2008; Dubois *et al.*, 2013; Van den  
92 Broeck *et al.*, 2017). This results in decreased levels of gibberellin and DELLA protein  
93 stabilisation, which pushes the cells to permanently exit the cell division phase and into the  
94 cell differentiation phase (Claeys *et al.*, 2012). The first transcriptional changes occur very  
95 rapidly, after 40 minutes of stress. However, early signalling and associated phosphorylation  
96 events that precede part of these transcriptional changes are largely unknown, likely because  
97 most phosphoproteomic studies focused on severe, lethal stress or on whole seedlings,  
98 masking the growth-specific phosphorylation events (Bhaskara *et al.*, 2017a).

99           While the transcriptional events orchestrating leaf growth upon mild stress have been  
100 studied extensively, the early proteome and phosphoproteome changes are not yet fully  
101 understood. In this study, we performed full proteome and phosphoproteome analyses on  
102 growing leaf tissue exposed to mannitol-induced stress and captured the rapid (within the first  
103 half hour) events associated with this stress. We demonstrate differences in proteome changes  
104 in the early (30 min) and later (4 h) mannitol-triggered proteome, such as the translational  
105 machinery and oxidation-reduction processes. Next, we evaluated the phosphoproteome and  
106 found several connections with the GA–DELLA pathway, which form interesting candidates  
107 for follow-up studies. We compared four phosphoproteome datasets after mild and severe  
108 stress highlighting their distinct signalling pathways. Finally, through validation of some  
109 candidates for a growth phenotype upon mild mannitol treatment, we identified H(+)-  
110 ATPASE 2 (AHA2) and CYSTEINE-RICH REPEAT SECRETORY PROTEIN 38  
111 (CRRP38) as novel regulators of osmotic stress signalling and response.

112

## 113 **MATERIAL AND METHODS**

114

### 115 **Plant material and growth conditions**

116

117 Wild-type plants (Col-0) were grown *in vitro* at 21°C under a 16-h-day (110 mmol/(m<sup>2</sup>s)) and  
118 8-h-night regime. 64 wild-type seeds were sown on a 14-cm-diameter Petri dish with solid ½  
119 MS medium (Murashige and Skoog, 1962; 6.5 g/L agar, Sigma), overlaid with a nylon mesh  
120 (Prosep) of 20-µm pore size. During growth, plates were randomized. For the short-term (30  
121 min mannitol stress) proteome and phosphoproteome analyses, half of the plants were  
122 transferred to ½ MS medium containing 25 mM mannitol (Sigma) at 15 days after  
123 stratification (DAS). The third leaf was harvested after 30 min. The other half of the plants

124 was not transferred, and the third leaf was harvested before transfer (time point 0). In total, 4  
125 biological repeats were performed. For the proteomic experiment after 4 h of mannitol stress  
126 and the expression analysis, half of the plants were transferred to control ½ MS medium, the  
127 other half to ½ MS medium containing 25 mM mannitol at 15 DAS. The third leaf was  
128 harvested 20 min and 40 min (for expression analysis) or 4 h (for proteomics) after transfer.  
129 In total 3 biological replicates were performed, and approximately 100 mg leaf material was  
130 harvested per sample. All experiments were performed independently.

131

### 132 **qPCR analyses**

133

134 Samples were immediately frozen in liquid nitrogen and ground with a Retsch machine and  
135 3-mm metal beads. Subsequently, RNA was extracted with TriZol (Invitrogen) and further  
136 purified with the RNeasy plant mini kit (Qiagen). For cDNA synthesis, the iScript  
137 cDNASynthesis Kit (Bio-Rad) was used with 1 µg of RNA as starting material. qRT-PCR  
138 was performed with the LightCycler 480 Real-Time SYBR Green PCR System (Roche). The  
139 data were normalised against the average of housekeeping genes AT1G13320 and  
140 AT2G28390 (Czechowski, 2005), as follows:  $dCt = Ct(\text{gene}) - Ct(\text{average [housekeeping} \\ 141 \text{ genes]})$  and  $ddCt = dCt(\text{Control}) - dCt(\text{Treatment})$ . Ct represents the number of cycles at  
142 which the SYBR Green fluorescence reached a threshold during the exponential phase of  
143 amplification. Primers were designed with Primer-BLAST  
144 (<https://www.ncbi.nlm.nih.gov/tools/primer-blast/>) (**Supplementary Information**).

145

### 146 **(Phospho)proteome workflow**

147

148 Plant material was flash-frozen in liquid nitrogen and ground into a fine powder. Subsequent  
149 proteome and phosphoproteome analyses were performed as previously described (Vu *et al.*,  
150 2016; Nikonorova *et al.*, 2018). For details, we refer to the **Supplementary Information**.  
151 LC-MS/MS analysis was performed as previously described (Vu *et al.*, 2016). Both the  
152 proteome and phosphoproteome samples were analysed using 3 h gradients on a quadrupole  
153 Orbitrap instrument (Q Exactive).

154 MS/MS spectra were searched against the Arabidopsis proteome database (TAIR10,  
155 containing 35,386 entries; <http://www.arabidopsis.org/>) using the MaxQuant software  
156 (version 1.5.4.1). Details on settings can be found in **Supplementary Information**. All MS  
157 proteomics data have been deposited to the ProteomeXchange Consortium via the PRIDE  
158 partner repository with the data set identifier PXD008900. For the quantitative proteome and  
159 phosphoproteome analyses, the “ProteinGroups” and ‘Phospho(STY)sites’ output files,  
160 respectively, generated by the MaxQuant search were loaded into Perseus software. For  
161 phosphoproteome data only high-confidence hits with phosphorylation localisation  
162 probability  $> 0.75$  were included in analysis. Data analysis was performed as described  
163 previously (Vu *et al.*, 2016), and modifications are added in the main text.

164

### 165 *In silico analyses, data visualisation and statistics*

166

167 To generate networks for known and predicted protein-protein interactions, the datasets were  
168 loaded to the STRING database (<https://string-db.org>; version 10.5) using high confidence  
169 interaction score ( $> 0.7$ ). As active interaction sources text mining, experiments, databases,  
170 co-expression, neighbourhood, gene fusion and co-occurrence were selected.  
171 (Phospho)proteins that did not have any interaction were removed from the network.  
172 Biological Process terms were retrieved from the TAIR portal ([www.arabidopsis.org](http://www.arabidopsis.org), Bulk

173 Data Retrieval). Further data visualisation was performed in Cytoscape (version 3.5.1) on the  
174 extracted interaction network and GO annotations. GO-enrichment analysis was performed in  
175 PLAZA 4.0 workbench using entire species as background model and 0.05 as a p-value cut-  
176 off. The HMMER web server was used for the prediction of kinase domains. For Motif-X  
177 analyses (Chou and Schwartz, 2011), the sequences (limited to 13 amino acids) of up- and  
178 downregulated phosphosites were pre-aligned with the phosphosite centered. The IPI  
179 Arabidopsis Proteome was used as the background database. The occurrence threshold was  
180 set at the minimum of 5 peptides, and the p-value threshold was set at  $<10^{-6}$ . Venn diagrams  
181 were created using the Venny 2.1 online tool (<http://bioinfogp.cnb.csic.es/tools/venny>).  
182 Barcharts, boxplots and statistical analyses for qPCR and phenotyping data were performed  
183 using R software (<https://www.R-project.org>) and all figures were generated with Inkscape or  
184 Photoshop. Details on ANOVA results can be found in **Supplementary Information**.

185

## 186 **Genotyping**

187

188 The *crrsp38-1* (SALK\_151902) and *aha2-4* (SALK\_082786) mutant *Arabidopsis* plants were  
189 obtained from Nottingham Arabidopsis Stock Centre (NASC). The homozygous *Arabidopsis*  
190 mutants were identified by PCR using primers specific to the insertion T-DNA  
191 (**Supplementary Information**) and the LB primer (ATTTTGCCGATTTTCGGAAC). The  
192 SALK lines used are in Col-0 background.

193

## 194 **Leaf growth phenotyping**

195

196 Both wild-type (Col-0) and mutant plants were grown *in vitro* on 14-cm-diameter Petri dishes  
197 at 21°C under a 16-h-day (110 mmol/(m<sup>2</sup>s)) and 8-h-night regime. The mutant line was



198 grown together with the appropriate control on one plate to correct for plate effects. For each  
199 condition (MS or mannitol), 4-6 plates with 8 wild-type and 8 mutant seeds per plate were  
200 sown. Half of the plants were grown on solid (9 g/L agar, Sigma) ½ MS control medium and  
201 the other half on solid ½ MS medium with the addition of 25 mM D-mannitol (Sigma). In  
202 total, 1 and 2 independent experiments were performed for *aha2-4* and *crrsp38*, respectively.  
203 The plates were photographed at 22 DAS and all images were analysed using ImageJ  
204 (Schindelin *et al.*, 2015) to measure the projected rosette area.

205

## 206 **RESULTS AND DISCUSSION**

207

### 208 *Proteome and phosphoproteome profiling to unravel the early mannitol response*

209

210 To gain insight in the early molecular changes associated with mannitol-triggered osmotic  
211 response, we focused on changes in the proteome and phosphoproteome in expanding leaf  
212 tissue of *Arabidopsis thaliana*. We opted for low concentrations of the osmoticum mannitol  
213 (25 mM), which enabled a mild stress that does not affect plant survival but solely represses  
214 growth (Skiryycz *et al.*, 2011a; Claeys *et al.*, 2014). Specifically, *A. thaliana* seedlings at 15  
215 days after stratification (DAS) were transferred to ½ MS medium containing 25 mM mannitol  
216 and after 30 min, the third expanding leaf was harvested in 4 biological repeats. We chose the  
217 30 min time point because this time point coincides with the earliest changes observed in the  
218 transcriptome data on mild osmotic stress in growing leaves (Van den Broeck *et al.*, 2017).  
219 Next, proteins were extracted and used for two parallel analyses: (i) the total proteome,  
220 enabling us to identify key proteins responding to mannitol, and (ii) the phosphoproteome,  
221 allowing us to gain insights into the early phosphorylation events. The proteome analysis of  
222 control and mannitol-treated samples resulted in total in the identification of 2932 protein

223 groups (a protein group includes proteins that cannot be unambiguously identified by unique  
224 peptides but have only shared peptides) (**Figure 1 and Supplementary Table S1**). The  
225 phosphoproteome analysis led to the identification of 3698 phosphorylated peptides that  
226 could be mapped on 1466 proteins (**Figure 1 and Supplementary Table S2**). In this list of  
227 identified phosphopeptides, the contributions of pS, pT, and pY were 82.2%, 17.0%, and  
228 0.8%, respectively (**Figure 1**). To address if the early mannitol-triggered leaf proteome is  
229 significantly different from a more long-term exposure, we also performed a 4 h mannitol  
230 treatment. This time point was chosen as it is 2 h later than the maximum in expression of  
231 several key transcription factors that were previously identified (Van den Broeck *et al.*,  
232 2017). The third expanding leaf was harvested in 3 biological replicates and led to  
233 identification of 2633 proteins (**Figure 2 and Supplementary Table S3**).

234

### 235 *Data filtering approach to identify relevant candidates for further studies*

236

237 One of the challenges in quantitative proteomics is dealing with missing data (Karpievitch *et*  
238 *al.*, 2012; Lazar *et al.*, 2016), which cannot be processed using standard regression methods  
239 (e.g., t-test and ANOVA). To overcome this, missing values can be imputed or ignored  
240 (Karpievitch *et al.*, 2012). However, this can lead to a misinterpretation of results and, more  
241 importantly, to the loss of potentially interesting proteins or phosphosites for further studies  
242 (Lazar *et al.*, 2016). A protein or a phosphorylated peptide that is present in a treated sample  
243 and absent in the control conditions (“one-state” or “unique” proteins or phosphopeptides,  
244 hereafter referred to as unique) and vice versa could be of great biological interest.

245 To date, post-Mass Spectrometry (MS) data analysis remains a highly debated field  
246 with numerous imputation techniques and sophisticated statistical approaches that aim to deal  
247 with a complete dataset with missing values (Koopmans *et al.*, 2014; Lazar *et al.*, 2016;

248 Wang *et al.*, 2017b). Here, to overcome the problem of missing values without imputation or  
249 complex statistical analysis, we applied a hybrid approach for data analysis that treats  
250 intensity-based and presence/absence data separately (**Figures 1 and 2 and Supplementary**  
251 **Figure 1**). The original, complete dataset containing  $\log_2$ -transformed intensities was split in  
252 three subsets (**Supplementary Figure 1; see Supplementary Information for details**).  
253 Dividing the dataset in three subsets allowed us to minimise the number of missing values in  
254 the input for regression analysis (subset 1), eliminate unreliable detections or quantifications  
255 (subset 2) and include unique proteins or phosphopeptides (subset 3) (**Figures 1 and 2,**  
256 **Supplementary Figure 1 and Supplementary Tables S1-3**). The follow-up statistical  
257 workflow was performed as described previously (Vu *et al.*, 2016). In brief, the dataset was  
258 centred around zero by a subtraction of the medium within each replicate and subjected to a  
259 two-sample t-test ( $p < 0.05$ ) (**Figures 1 and 2**).

260

### 261 *Early (30 min) mannitol-triggered effects on the leaf proteome*

262

263 For the proteome analysis, the above-described approach resulted in 18 and 21 unique  
264 proteins detected only in the control and mannitol-treated sample, respectively (**Figure 1 and**  
265 **Supplementary Table S1**). In addition, statistical analysis determined 128 differentially  
266 abundant proteins: 27 higher and 101 that were found lower in abundance upon mannitol  
267 treatment compared to the control (**Figure 1 and Supplementary Table S1**). To simplify  
268 data characterisation further, we arranged proteins in two groups: upregulated (proteins  
269 detected only in mannitol-treated samples and significantly more abundant upon mannitol  
270 treatment) and downregulated (proteins detected only in control samples and significantly  
271 more abundant in control conditions).

272 Using the PLAZA 4.0 platform, GO enrichment analysis was conducted on the dataset  
273 in the context of biological process (**Supplementary Table S4**). GO enrichment on  
274 biological processes showed that differentially regulated proteins (including unique ones)  
275 were involved in various processes, such as response to stress and abiotic stimulus.

276 To better understand the relationships between the 167 up- and down-regulated  
277 proteins, we constructed a protein-protein interaction network consisting of 105 interacting  
278 proteins with 242 (potential) interactions (see Material and Methods for details). To get  
279 insight into the early biological processes affected by mild osmotic stress, GO annotations of  
280 up- and down-regulated proteins were superimposed on the network and nodes were grouped  
281 accordingly (**Figure 3**). This approach revealed that most interacting proteins were involved  
282 in protein metabolism, specifically in amino acid biosynthesis, translation and ribosome  
283 biogenesis, protein folding, intracellular protein transport and ubiquitin-dependent protein  
284 degradation.

285 In a first large group of differentially abundant interacting proteins, we observed that  
286 ribosomal proteins were highly regulated upon mannitol exposure, suggesting an altered  
287 capacity for protein translation. Six ribosomal proteins were unique for the mannitol  
288 treatment and two were upregulated. This is in line with the observation of long-term  
289 proteome changes in growing Arabidopsis leaves subjected to mannitol, where the levels of  
290 ribosomal and translational proteins were also found highly regulated, both up and  
291 downregulated (Skirycz *et al.*, 2011b).

292 A second large group of proteins in our network was involved in oxidation-reduction  
293 processes and biotic and abiotic stress responses. CAT1 was detected as a unique protein for  
294 the mannitol-treated samples, most likely protecting plant cells against toxic effects of ROS  
295 produced upon osmotic stress. Surprisingly, other reduction-oxidation protein family  
296 members (2 glutathion peroxidases, 2 ascorbate peroxidases and 9 thioredoxines, 1

297 periredoxin, 1 glutaredoxin and 1 dehydro-ascorbate reductase) appeared to be  
298 downregulated. This is in contrast with the long-term proteome changes in growing leaf  
299 tissue (Skirycz *et al.*, 2011b) and not expected because peroxidases have been widely  
300 described as ROS scavengers and are involved in the ROS damage repair (Kapoor and  
301 Sveenivasan, 1988; Caverzan *et al.*, 2012; Bela *et al.*, 2015). ROS are known to play a dual  
302 role: being toxic and destructive molecules, but, they can also serve as signalling molecules  
303 regulating stress responses, growth and development (Kovtun *et al.*, 2000; Foyer and Noctor,  
304 2005; Vanderauwera *et al.*, 2005; Gadjev *et al.*, 2006; Pitzschke and Hirt, 2006; Brown and  
305 Griendling, 2009; Hossain *et al.*, 2015). The downregulation of these scavenger proteins  
306 might be a result of the lack of ROS production during the very early stages of mild osmotic  
307 stress or because these enzymes are a source of hydrogen peroxide (H<sub>2</sub>O<sub>2</sub>) (Blokhina *et al.*,  
308 2003). The first hypothesis is in line with the observation that H<sub>2</sub>O<sub>2</sub> levels do not accumulate  
309 within the first 10 min upon a hyperosmotic treatment and even decrease to levels lower than  
310 the control at later time points in Arabidopsis cell cultures (Beffagna *et al.*, 2005). On a  
311 transcript level, glutathione peroxidases have already been shown to be downregulated in rice  
312 upon drought stress (Passaia *et al.*, 2013). Deficiency in some ROS scavengers led to an  
313 increase in the plant's sensitivity to oxidative stress while exposure to osmotic and salt  
314 stresses resulted in an increased tolerance (Miller *et al.*, 2007).

315         The third largest cluster in the network consisted of proteins related to photosynthesis  
316 and carbohydrate metabolism. Members of this group were mainly downregulated under  
317 mannitol stress except for a phosphoenolpyruvate carboxylase family protein (PEPC,  
318 AT1G77060). This is in agreement with previous studies where it was shown that abiotic  
319 stresses can induce *PEPC* gene expression in wheat, Arabidopsis and sorghum (Echevarría *et*  
320 *al.*, 2001; González *et al.*, 2003; García-Mauriño *et al.*, 2003; Sánchez *et al.*, 2006).  
321 Moreover, recent studies demonstrated that the maize *PEPC* gene was able to confer drought

322 tolerance and increase grain yield in transgenic wheat plants (Qin *et al.*, 2016).  
323 Photosynthesis-related proteins, such as PHOTOSYSTEM II SUBUNIT Q and  
324 PHOTOSYSTEM II SUBUNIT P, were downregulated upon mannitol-induced stress, as  
325 were many chloroplast-located proteins (18 of the 121) (Lawlor and Tezara, 2009). This was  
326 expected as the photosynthetic electron transfer chain can produce ROS species  
327 (Ramachandra Reddy *et al.*, 2004).

328 Another interesting protein identified as unique for mannitol-treated samples was  
329 SUPER SENSITIVE TO ABA AND DROUGHT 2 (SAD2)/ ENHANCED MIRNA  
330 ACTIVITY 1 (EMA1) (**Supplementary Table S1**), an importin protein that regulates nuclear  
331 transport and is involved in the regulation of miRNA's (Verslues *et al.*, 2006b; Wang *et al.*,  
332 2011). *SAD2/EMA1* is transcriptionally not induced by ABA and stress treatments, but  
333 mutant lines show a hypersensitivity to ABA treatment and salt stress (Verslues *et al.*,  
334 2006b).

335 To conclude, our results point towards a downregulation of photosynthesis and  
336 upregulation of CAT1 probably for ROS scavenging, both systems potentially reduce ROS  
337 production. In addition, our results suggest an unexpected new role for peroxidases in the  
338 early mannitol response as these were downregulated.

339

#### 340 ***Lack of correlation between early mannitol-triggered transcript and protein fold changes***

341

342 Because some proteins are mainly regulated at post-transcriptional level, such as the above-  
343 mentioned EMA1, we evaluated to what extent changes in transcript abundance for a  
344 selection of 14 genes correlated with protein levels. For this, expanding leaf tissue (leaf 3, 15  
345 days after sowing) was harvested 20 and 40 min after mild mannitol treatment. We included  
346 the genes with the highest change in protein abundance and some of the unique proteins.

347 Surprisingly, we found almost no obvious changes after 20 and 40 min of mannitol treatment  
348 at the transcriptional level for the genes (**Figure 4**). This suggested that changes in protein  
349 levels at 30 min were not caused by changes in transcript abundance, but more likely due to  
350 differences in protein degradation or stabilisation. We concluded that even though the  
351 transcript level was tested for only a subset of proteins, the transcriptome poorly reflects the  
352 proteome, which is in agreement with other studies (Jogaiah *et al.*, 2013; Bai *et al.*, 2015;  
353 Walley *et al.*, 2016).

354

### 355 *Effects of four hours mannitol treatment on the leaf proteome*

356

357 To get an idea on changes in protein abundance upon more prolonged mild osmotic stress, we  
358 also performed a proteome analysis of growing leaf tissue after 4 hours of mannitol  
359 treatment. The above described data analysis workflow led to the identification of 15 unique  
360 proteins (based on absence or presence in 3 out of 3 biological replicates), 14 for the control  
361 and one for the mannitol-treated sample. Together with the statistical analysis, this resulted in  
362 83 differentially abundant proteins (49 more abundant and 34 less abundant upon stress)  
363 (**Figure 2 and Supplementary Table S3**). GO enrichment on biological processes showed  
364 that differentially regulated proteins (including unique ones) were, among several others,  
365 involved in response to stress and to abiotic stimulus (**Supplementary Table S4**). A protein-  
366 protein interaction network was built for up- and downregulated proteins (see Material and  
367 Methods for details), and similar to 30 min mannitol treatment, the vast majority of  
368 interacting proteins was involved in translation and ribosome biogenesis (**Figure 5**).

369 To unravel dynamic changes of proteins that were up- and downregulated at 30 min,  
370 we traced these proteins in the 4 h mannitol dataset. Despite that we cannot compare the  
371 exact values from both experiments, as they were processed separately, we can make some

372 assumptions based on the protein fold changes. Thus, 167 up- and downregulated proteins of  
373 the 30 min dataset were mapped on the total 4 h proteome data and 120 proteins were  
374 retained (**Figure 6 and Supplementary Table S5**). However, only 6 of these proteins were  
375 significantly differentially abundant after 4 h (**Supplementary Table S3**). Of the 120  
376 mapped proteins 59 proteins showed the same trend at 30 min and 4 h after mannitol  
377 treatment of which 16 proteins remained upregulated and 43 proteins downregulated. This  
378 group of “stable” proteins contained various reduction-oxidation proteins, such as 5  
379 thioredoxins, 2 peroxiredoxins, 1 ascorbate peroxidase, 1 glutathione peroxidase, 1  
380 superoxide dismutase (SOD1) and 1 catalase (CAT1). Another group of proteins, consisting  
381 of 11 proteins, was upregulated at 30 minutes and downregulated after 4 h of mannitol  
382 treatment. The group of proteins that were downregulated at 30 minutes and became  
383 upregulated after 4 h of mannitol treatment included 50 proteins with diverse functions.  
384 Overall, these observations suggested a dynamic control of protein levels during mild  
385 osmotic stress response.

386

### 387 *Early (30 min) mannitol-triggered effects on the leaf phosphoproteome*

388

389 In the phosphoproteome analysis, 96 unique phosphorylated peptides were detected – 56 and  
390 40 for control and mannitol-treated samples, respectively (**Figure 1 and Supplementary**  
391 **Table S2**). The statistical workflow resulted in a list of 76 differentially abundant  
392 phosphopeptides: 40 higher and 36 lower in abundance upon mannitol treatment compared to  
393 the control (**Figure 1 and Supplementary Table S2**). Similar as for the proteome data, we  
394 combined unique and differentially abundant phosphopeptides in two sets of upregulated and  
395 downregulated proteins and subjected them to further analyses.



396 GO analysis of biological process terms revealed that proteins with differentially  
397 regulated phosphosites under mild osmotic stress (including unique phosphosites) were  
398 involved in several processes, including (protein) phosphorylation, regulation of cellular  
399 response to stress, response to abscisic acid and mannitol metabolic process (**Supplementary**  
400 **Table S4.**).

401 To unravel possible interactions between the proteins that were differentially  
402 phosphorylated and unique, we constructed, as for the proteome datasets, a protein-protein  
403 interaction network consisting of 44 interacting phosphoproteins with 42 (potential)  
404 interactions combined with GO categorisation for biological processes (see Material and  
405 Methods for details). This approach revealed that interacting phosphoproteins were mainly  
406 involved in photosynthesis, splicing, chromatin remodelling and transport (**Figure 7**). In  
407 general, this network analysis showed that 27% of the detected phosphoproteins are part of a  
408 subnetwork, suggesting that upon a stimulus, more than one protein of the subnetwork is  
409 differentially phosphorylated, potentially affecting its activity. However, it should be noted  
410 that we cannot pinpoint a role for the identified change in phospho-status in relation to the  
411 protein function or activity.

412 Upon mild osmotic stress, the DELLA proteins play an important role in the growth  
413 inhibition in leaves upon mild osmotic stress (Claeys *et al.*, 2012). GA binds to its receptor  
414 GA INSENSITIVE DWARF1 (GID1) (Ueguchi-Tanaka *et al.*, 2005) and forms a complex  
415 with DELLA proteins, leading to its degradation (Nakajima *et al.*, 2006). Under mild stress,  
416 the gene encoding a GA-degradation enzyme, *GA2-OX6*, is upregulated by several mannitol-  
417 responsive transcription factors (Van den Broeck *et al.*, 2017), which leads to a decrease in  
418 GA levels and subsequently to the stabilisation of DELLA proteins. Such stabilisation of  
419 DELLA proteins leads to changes in the activity of transcription factors and expression of  
420 GA-regulated genes. In our phosphoproteomic dataset, we found a few differentially

421 phosphorylated proteins that are linked to DELLAs. For example, bZIP16 (AT2G35530;  
422 Ser<sup>152</sup>, >1.5-fold downregulated) (**Table 1**), a transcriptional repressor, has been shown to  
423 directly repress *REPRESSOR OF GA-LIKE 2 (RGL2)*, encoding a DELLA protein (Hsieh *et*  
424 *al.*, 2012). We thus hypothesize that a decrease in phosphorylation of bZIP16 might decrease  
425 its activity and its repression on *RGL2*. Another example is the CALCIUM-DEPENDENT  
426 PROTEIN KINASE (CDPK/CPK)-RELATED PROTEIN KINASE 2 (TAGK2/CRK2)  
427 (AT3G19100), for which a phospho-site at Ser<sup>57</sup> was upregulated 1.6-fold upon mannitol  
428 treatment (**Table 1**). Recently it was shown that TAGK2/CRK2 phosphorylates the GA  
429 RECEPTOR RING E3 UBIQUITIN LIGASE (GARU) at Tyr<sup>321</sup> which results in the  
430 disruption of the interaction between GARU and the GA RECEPTOR GA INSENSITIVE  
431 DWARF1 (GID1). Because this interaction is disrupted, GARU is not able to induce the  
432 degradation of GID1. *TAGK2*-overexpressing plants thus show an increased GID1  
433 stabilisation and DELLA degradation (Nemoto *et al.*, 2017). However, the role of  
434 phosphorylation associated with TAGK2 has not yet been studied.

435         Considering the interest in early signalling cascades underlying responses to mild  
436 osmotic stress, we focused on proteins with up- and downregulated phosphosites possessing  
437 protein kinase activity. Using the HMMER online tool (Finn *et al.*, 2015), we found 7 and 10  
438 (potential) protein kinases of which phosphosites were up- and downregulated, respectively  
439 (**Supplementary Table S6**). Upregulation of phosphorylation sites of a kinase can indicate  
440 an activation of the kinase itself and, as a consequence, its downstream signaling cascades;  
441 and dephosphorylation can imply the opposite (Wang *et al.*, 2007; Tarrant and Cole, 2009;  
442 Day *et al.*, 2016). Next, we looked into predicted overrepresented kinase motifs as the  
443 sequence consensus of phosphopeptide motifs reflects the kinase-specific regulation of  
444 substrate phosphorylation and the identity of the corresponding kinases (**Supplementary**  
445 **Figure S2**). This revealed that for the upregulated phosphopeptides, the protein motifs [SP]

446 and [TP] were the most enriched motifs. Peptides containing the proline (P)-directed [SP] and  
447 [TP] motifs are suggested to be targets of MAP-kinases, SnRK2, RLKs, CDPKs, CDKs,  
448 AGC family protein kinases and STE20-like kinases (van Wijk *et al.*, 2014). For the  
449 downregulated phosphopeptides, [SP] and [RxxS] motifs were overrepresented, of which the  
450 [RxxS] motif is recognized by MAP kinases.

451 Some examples of the identified kinases that have a changed phospho-status upon  
452 mild mannitol stress are CALCINEURIN B-LIKE PROTEIN (CBL) - INTERACTING  
453 PROTEIN KINASE 8 (CIPK8, AT4G24400), MAP kinase kinase kinase 7 (MKKK7,  
454 AT3G13530), brassinosteroid-signalling kinase 1 (BSK1, AT4G35230) and SnRK2.4  
455 (AT1G10940) (**Table 1**). CIPKs are involved in calcium signalling cascades and are found to  
456 be induced in response to stress (Hu *et al.*, 2009; Pandey *et al.*, 2014). Mitogen activated  
457 protein kinase (MAPK) cascades are known to be involved in drought stress (Ichimura *et al.*,  
458 2000) and in PAMP signalling (Asai *et al.*, 2002; Pitzschke *et al.*, 2009). The detected  
459 MKKK7 was demonstrated as a negative regulator of flg22-triggered signalling and basal  
460 immunity (Mithoe *et al.*, 2016), but could have other functions as well. BSK1 is a target of  
461 the brassinosteroid receptor BRASSINOSTEROID INSENSITIVE 1 (BRI1) and plays a role  
462 in the brassinosteroid signalling during plant immunity (Shi *et al.*, 2013). SnRK2.4 is a well-  
463 known regulator of the salt stress response in plants. According to recent findings, SnRK2.4  
464 belongs to the SnRK2 group 1 of which its members are not activated by abscisic acid (ABA)  
465 (Kulik *et al.*, 2011). The importance of phosphorylation for SnRK2.4 activity was previously  
466 demonstrated upon salt stress and the abolishment of SnRK2.4 activity in mutant lines led to  
467 an increased sensitivity to salt (Krzywińska *et al.*, 2016). The first phase of salt stress is  
468 osmotic stress, strengthening a role for SnRK2.4 in this process (Shavrukov, 2013). However,  
469 our analysis showed a different mannitol-regulated phosphorylation site than those previously  
470 described (Kline *et al.*, 2010), namely Ser<sup>357</sup>. The Ser<sup>357</sup> residue was dephosphorylated upon

471 mannitol treatment, and is located in a protein-protein interaction motif outside the activation  
472 loop of the kinase that has not been linked to osmotic stress responses (Kulik *et al.*, 2011).

473

#### 474 *A normalised early mannitol-triggered differential leaf phosphoproteome*

475

476 A common question related to quantitative phosphoproteomics is whether the measured  
477 phosphorylation changes result from changes in kinase or phosphatase activity or from  
478 changes in phosphoprotein abundance. In the context of quantitative phosphoproteomics it is  
479 important to correct – to the extent possible – the measured phosphorylation changes with  
480 respect to changes in protein abundance (Vu *et al.*, 2016). Taking into account that  
481 phosphopeptide abundance is directly depending on protein abundance, we normalised  
482 phosphosite intensities. It should be noted that this analysis is only possible for a subset of  
483 identified phosphosites because as a result of the enrichment for phosphorylated proteins  
484 during the phosphoproteome analysis, most of them are not detected in the whole proteome  
485 where no enrichment was performed. Furthermore, it should be mentioned that this  
486 normalised phosphoproteome data set does not imply that the non-normalised  
487 phosphopeptides are not interesting to investigate; merely that these changes could not be  
488 corrected for protein abundance. 172 up- and downregulated phosphorylated peptides derived  
489 from 158 phosphoproteins were mapped on the total proteome data and 32 proteins were  
490 found to be overlapping. Next, the  $\log_2$  fold change of the protein was subtracted from the  
491  $\log_2$  fold change of the phosphosite. This defined a set of phosphorylation events that are  
492 fully due to changes in kinase and phosphatase activity and not due to changes in protein  
493 abundance (to the extent these changes in phosphorylation status do not impact on protein  
494 abundance) (**Figure 8 and Supplementary Table S7**). Sixteen phosphosites could not be  
495 normalised as they belonged to a group of unique phosphosites and did not have a fold

496 change value. Within the normalised phosphopeptides, two phosphosites of a remorin family  
497 member REM1.3 (AT2G45820), Thr<sup>58</sup> and Ser<sup>64</sup>, were down regulated upon mannitol  
498 treatment (**Figure 8 and Table 1**). REM1.3 was already reported to be phosphorylated upon  
499 oligo-galacturonide treatment which elucidates a plant stress response (Kohorn *et al.*, 2016).  
500 REM1.3 is proposed as a scaffolding protein for signalling at the plasma membrane and is  
501 thus an interesting candidate for mannitol-induced signalling (Marín *et al.*, 2012).

502

503 *Comparative phosphoproteome analysis identifies bZIP30 and RBB1 as general players in*  
504 *osmotic stress response*

505

506 To assess whether the mannitol-regulated phosphorylated proteins in growing leaf tissue are  
507 part of a more general stress response or are specific for the stress-induced growth-regulating  
508 response, we compared our data set (30 min 25 mM mannitol) with 3 previously published  
509 osmotic stress-related phosphoproteome datasets (Xue *et al.*, 2013; Stecker *et al.*, 2014;  
510 Bhaskara *et al.*, 2017b). Given the differences in experimental set-up (long-term versus short-  
511 term or mild versus severe stress) (see **Table 2** for details), we found little overlap between  
512 all four datasets; only two proteins, BASIC LEUCINE-ZIPPER 30 (BZIP30)/DRINK ME  
513 (DKM) and REGULATOR OF BULB BIOGENESIS1 (RBB1) (Han *et al.*, 2015), were  
514 detected in all datasets, possibly indicating a general role in osmotic stress responses (**Figure**  
515 **9 and Supplementary Table S8**). Interestingly, the same phosphorylation site, Ser<sup>176</sup>, of  
516 bZIP30 was found to be upregulated in the 3 datasets where mannitol was used. It should be  
517 noted that bZIP30 (Ser<sup>176</sup>, >1.5-fold upregulated, **Table 1**) was also identified in our network  
518 as a central phosphoprotein in the longest interaction chain (**Figure 7**). This transcription  
519 factor influences the expression of cell cycle and cell expansion genes, two processes that are  
520 affected by mild mannitol treatment (Skiryycz *et al.*, 2011b; Lozano-Sotomayor *et al.*, 2016).

521 In addition, we found 4 common mannitol-responsive phosphoproteins (based on overlap  
522 between (Xue *et al.*, 2013), (Stecker *et al.*, 2014) and this study). The phosphorylation site  
523 Ser<sup>680</sup> of VARICOSE-RELATED PROTEIN (VCR, AT3G13290) was identified as  
524 upregulated in all studies where mannitol was used. In addition, six phosphoproteins were  
525 exclusively found in the two mild osmotic stress studies (Bhaskara *et al.*, 2017a and this  
526 study), including a mitogen activated protein kinase kinase kinase-like protein (AT3G58640)  
527 and MPK3/6-TARGETED VQ MOTIF-CONTAINING PROTEIN 1 (MVQ1, AT1G28280).

528         Apart from the different methodologies, the limited overlap points out the large  
529 difference between short and long-term phosphorylation response upon stress, indicating the  
530 transient and dynamic behaviour of phosphorylation events. Additionally, the severity of the  
531 stress determines the phosphorylation response (Bhaskara *et al.*, 2017a).

532

533 *(Phospho) proteome profiling identifies AHA2 and CRRSP38 as growth regulators under*  
534 *mannitol stress*

535

536 To assess the involvement of proteins with a differential abundance or phosphorylation status  
537 in shoot growth and/or mannitol response, and thus the quality of our data set, we selected  
538 two candidates for phenotypic analysis. From the mannitol-regulated proteome data set  
539 (**Supplementary Table S1**), we selected the uncharacterized CYSTEINE-RICH REPEAT  
540 SECRETORY PROTEIN 38 (CRRSP38, AT3G22060). Interestingly this protein was  
541 identified as down-regulated after 30 min of mannitol application and was not detected after 4  
542 h of mannitol stress treatment. This is in contrast to the absence of any mannitol-induced  
543 transcriptional change at 20 and 40 min, and the increasing expression from 2 h on  
544 (**Supplementary Figure S4**). Possibly, this is due to a transcript - protein level feedback  
545 mechanism. We obtained a knock-out allele of CRRSP38 (SALK\_151902), referred to as

546 *crrsp38-1* (**Figure 10 and Supplementary Figure S3**). Phenotypic analyses of *crrsp38-1* at  
547 22 days after sowing revealed a larger rosette area both under control and mild mannitol  
548 conditions (**Figure 10**), suggesting that this protein is potentially a general growth regulator  
549 instead of specifically involved in the growth regulation upon mild stress. It will be  
550 interesting to explore the molecular function of CRRSP38 in leaf growth regulation, and its  
551 precise role upon mild mannitol-induced stress.

552 From the normalised phosphoproteome, we focused on AHA2 (AT4G30190), an  
553 H(+)-ATPASE 2 of which phosphosite Thr<sup>881</sup> showed a 1.9-fold increase in phosphorylation  
554 after mannitol treatment and had not yet been connected to mannitol stress, and does not  
555 show any obvious mannitol-induced transcriptional change in a time course experiment  
556 (**Figure 8, Supplementary Figure S4 and Supplementary Table S7**). Thr<sup>881</sup> is situated in  
557 the conserved autoinhibitory region I of the C-terminal domain of AHA2 (Rudashevskaya *et*  
558 *al.*, 2012; Falhof *et al.*, 2016), and rapid PLANT PEPTIDE CONTAINING SULFATED  
559 TYROSINE 1 (PSY1)-induced *in planta* phosphorylation of AHA2 at Thr<sup>881</sup> increases proton  
560 efflux (Fuglsang *et al.*, 2014). We hypothesized AHA2 might play a role in growth inhibition  
561 upon mild osmotic stress. Therefore, we characterized the strong knock-down *aha2-4* mutant  
562 with only about 10% AHA2 expression compared to wild type (Haruta *et al.*, 2010). As for  
563 *crrsp38-1*, the rosette area of the *aha2-4* mutant was measured at 22 DAS under normal and  
564 mild mannitol conditions. The *aha2-4* plants have a slightly larger rosette area in control  
565 conditions (8%) and were significantly more sensitive to mannitol compared to wild-type  
566 (**Figure 10**). Specifically, the *aha2-4* mutant showed a significant reduction of 59% under  
567 mannitol conditions compared to a reduction of 38% in the wild-type plants. This suggested  
568 that AHA2 can indeed regulate the mannitol-induced growth inhibition.

569 In summary, our (phospho)proteome-centred approach allowed the identification of  
570 novel mannitol stress-related players.

571

572

## 573 **CONCLUSIONS**

574

575 In this study, label-free proteomic and phosphoproteomic analyses were performed on  
576 expanding *Arabidopsis* leaves exposed to mild osmotic stress. By performing the proteome  
577 analysis at two different time points, 30 min and 4 h, dynamic patterns in protein abundance  
578 could be observed. In general, after 30 min of stress ribosomal proteins were upregulated  
579 upon mannitol treatment, and photosynthesis and reduction-oxidation-related proteins were  
580 downregulated. While after 4 h, ribosomal proteins were downregulated. Furthermore, the  
581 lack of correlation between transcriptional changes prior to changes in protein abundance  
582 points towards an important role of protein degradation/stabilisation upon stress. In addition,  
583 we identified several proteins that had an altered phosphorylation status upon mild osmotic  
584 stress, suggesting an important role for kinase and phosphatase-mediated signalling. We also  
585 identified several important regulators, such as the transcription factor bZIP30, which is  
586 likely a central component of both mild and severe osmotic stress. However, previously and  
587 in this study, no transcriptional changes were observed for bZIP30, indicating that by solely  
588 studying transcriptomics, central proteins involved in stress response are likely missed. On  
589 the other hand, several transcription factors from the recently described mild mannitol stress-  
590 associated gene regulatory network were not identified in our (phospho)proteomes. In  
591 addition, we identified proteins that were specifically phosphorylated under short-term mild  
592 osmotic stress, such as AHA2. Phenotypic analysis of an *aha2* knock-out mutant indeed  
593 confirmed a role for AHA2 in the regulation of growth upon mild osmotic stress.



594 Taken together, our datasets further stress the importance of proteome- and  
595 phosphoproteome-based approaches, in addition to transcriptomics, for unravelling the  
596 molecular mechanisms underlying growth regulation under stress.

597

598

599

## 600 **SUPPLEMENTARY DATA**

601

### 602 **Supplementary Information**

603 **Supplementary Figure S1.** Visual explanation for the 3 subsets described in the main text.

604 **Supplementary Figure S2.** Visual depiction of predicted overrepresented kinase motifs  
605 based on Motif X analysis.

606 **Supplementary Figure S3.** Details of *crrsp38-1* T-DNA line.

607 **Supplementary Table S1.** Proteins identified at 30 min after mannitol treatment, including  
608 raw data, differentially abundant and unique proteins.

609 **Supplementary Table S2.** Phosphosites identified at 30 min after mannitol treatment,  
610 including raw data, differentially abundant and unique phosphosites.

611 **Supplementary Table S3.** Proteins identified at 4 h after mannitol treatment, including raw  
612 data, differentially abundant and unique proteins.

613 **Supplementary Table S4.** GO enrichment on biological processes.

614 **Supplementary Table S5.** Comparative analysis of proteome datasets from 30 min  
615 (significantly different and unique proteins) and 4 h (all dataset) mannitol treatment.

616 **Supplementary Table S6.** Protein kinases with differentially phosphorelated and unique  
617 phosphosites predicted by HMMER.

618 **Supplementary Table S7.** Phosphorylated proteins normalised for protein abundance.

619 **Supplementary Table S8.** Comparative analysis of outputs from 4 phosphoproteomic  
620 studies on osmotic stress.

621

622

623

624

## 625 **ACKNOWLEDGEMENTS**

626

627 We thank Lam Dai Vu and Veronique Storme for valuable discussions. L.V.d.B. is a  
628 predoctoral fellow of the Research Foundation Flanders (FWO no. 131013). This research  
629 received funding from the Bijzonder Onderzoeksfonds Methusalem Project  
630 (BOF08/01M00408).

631

## 632 **REFERENCES**

633

- 634 **Aguirrezabal L, Bouchier-Combaud S, Radziejowski A, Dauzat M, Cookson SJ,**  
635 **Granier C.** 2006. Plasticity to soil water deficit in *Arabidopsis thaliana*: dissection of leaf  
636 development into underlying growth dynamic and cellular variables reveals invisible  
637 phenotypes. *Plant, cell & environment* **29**, 2216–27.
- 638 **Asai T, Tena G, Plotnikova J, Willmann MR, Chiu W, Gomez-gomez L, Boller T,**  
639 **Ausubel FM, Sheen J.** 2002. MAP kinase signalling cascade in *Arabidopsis* innate  
640 immunity. *Nature* **415**, 977–983.
- 641 **Bac-Molenaar JA, Granier C, Keurentjes JJB, Vreugdenhil D.** 2016. Genome-wide  
642 association mapping of time-dependent growth responses to moderate drought stress in  
643 *Arabidopsis*. *Plant, cell & environment* **39**, 88–102.

- 644 **Bai Y, Wang S, Zhong H, Yang Q, Zhang F, Zhuang Z, Yuan J, Nie X, Wang S.** 2015.  
645 Integrative analyses reveal transcriptome-proteome correlation in biological pathways and  
646 secondary metabolism clusters in *A. flavus* in response to temperature. *Scientific Reports* **5**,  
647 1–13.
- 648 **Beffagna N, Buffoli B, Busi C.** 2005. Modulation of reactive oxygen species production  
649 during osmotic stress in *Arabidopsis thaliana* cultured cells: involvement of the plasma  
650 membrane Ca<sup>2+</sup>-ATPase and H<sup>+</sup>-ATPase. *Plant & cell physiology* **46**, 1326–39.
- 651 **Bela K, Horváth E, Gallé Á, Szabados L, Tari I, Csiszár J.** 2015. Plant glutathione  
652 peroxidases: Emerging role of the antioxidant enzymes in plant development and stress  
653 responses. *Journal of Plant Physiology* **176**, 192–201.
- 654 **Berens ML, Berry HM, Mine A, Argueso CT, Tsuda K.** 2017. Evolution of Hormone  
655 Signaling Networks in Plant Defense. *Annual Review of Phytopathology* **55**, 401–425.
- 656 **Bhaskara GB, Nguyen TT, Yang T-H, Verslues PE.** 2017a. Comparative Analysis of  
657 Phosphoproteome Remodeling After Short Term Water Stress and ABA Treatments versus  
658 Longer Term Water Stress Acclimation. *Frontiers in Plant Science* **8**, 1–7.
- 659 **Bhaskara GB, Wen T-N, Nguyen TT, Verslues PE.** 2017b. Protein Phosphatase 2Cs and  
660 *Microtubule-Associated Stress Protein 1* Control Microtubule Stability, Plant Growth, and  
661 Drought Response. *The Plant Cell* **29**, 169–191.
- 662 **Blokhina O, Virolainen E, Fagerstedt K V.** 2003. Antioxidants, Oxidative Damage and  
663 Oxygen Deprivation Stress: a Review. *Annals of Botany* **91**, 179–194.
- 664 **Boyer JS.** 1982. Plant Productivity and Environment. *Science* **218**, 443–448.
- 665 **Van den Broeck L, Dubois M, Vermeersch M, Storme V, Matsui M, Inzé D.** 2017. From  
666 network to phenotype: the dynamic wiring of an *Arabidopsis* transcriptional network induced  
667 by osmotic stress. *Molecular systems biology* **13**, 961.
- 668 **Brown DI, Griendling KK.** 2009. Nox proteins in signal transduction. *Free radical biology*

- 669 & medicine **47**, 1239–53.
- 670 **Caverzan A, Passaia G, Rosa SB, Ribeiro CW, Lazzarotto F, Margis-Pinheiro M.** 2012.
- 671 Plant responses to stresses: Role of ascorbate peroxidase in the antioxidant protection.
- 672 Genetics and Molecular Biology **35**, 1011–1019.
- 673 **Chou MF, Schwartz D.** 2011. Biological Sequence Motif Discovery Using motif-x. Current
- 674 Protocols in Bioinformatics. Hoboken, NJ, USA: John Wiley & Sons, Inc., 1–24.
- 675 **Claeys H, Van Landeghem S, Dubois M, Maleux K, Inzé D.** 2014. What Is Stress? Dose-
- 676 Response Effects in Commonly Used in Vitro Stress Assays. Plant physiology **165**, 519–527.
- 677 **Claeys H, Skirycz A, Maleux K, Inze D.** 2012. DELLA Signaling Mediates Stress-Induced
- 678 Cell Differentiation in Arabidopsis Leaves through Modulation of Anaphase-Promoting
- 679 Complex/Cyclosome Activity. PLANT PHYSIOLOGY **159**, 739–747.
- 680 **Clauw P, Coppens F, De Beuf K, Dhondt S, Van Daele T, Maleux K, Storme V, Clement**
- 681 **L, Gonzalez N, Inzé D.** 2015. Leaf responses to mild drought stress in natural variants of
- 682 Arabidopsis. Plant physiology **167**, 800–16.
- 683 **Clauw P, Coppens F, Korte A, et al.** 2016. Leaf Growth Response to Mild Drought: Natural
- 684 Variation in Arabidopsis Sheds Light on Trait Architecture. The Plant cell **28**, 2417–2434.
- 685 **Czechowski T.** 2005. Genome-Wide Identification and Testing of Superior Reference Genes
- 686 for Transcript Normalization in Arabidopsis. PLANT PHYSIOLOGY **139**, 5–17.
- 687 **Day EK, Sosale NG, Lazzara MJ.** 2016. Cell signaling regulation by protein
- 688 phosphorylation: A multivariate, heterogeneous, and context-dependent process. Current
- 689 Opinion in Biotechnology **40**, 185–192.
- 690 **Demarsy E, Goldschmidt-Clermont M, Ulm R.** 2017. Coping with ‘Dark Sides of the Sun’
- 691 through Photoreceptor Signaling. Trends in plant science, 1–12.
- 692 **Dubois M, Claeys H, Van den Broeck L, Inzé D.** 2017. Time of day determines
- 693 Arabidopsis transcriptome and growth dynamics under mild drought. Plant, cell &

694 environment **40**, 180–189.

695 **Dubois M, Skirycz A, Claeys H, et al.** 2013. Ethylene Response Factor6 acts as a central  
696 regulator of leaf growth under water-limiting conditions in Arabidopsis. *Plant physiology*  
697 **162**, 319–32.

698 **Echevarría C, García-Mauriño S, Alvarez R, Soler A, Vidal J.** 2001. Salt stress increases  
699 the Ca<sup>2+</sup>-independent phosphoenolpyruvate carboxylase kinase activity in Sorghum leaves.  
700 *Planta* **214**, 283–287.

701 **Falhof J, Pedersen JT, Fuglsang AT, Palmgren M.** 2016. Plasma Membrane H(+)-ATPase  
702 Regulation in the Center of Plant Physiology. *Molecular plant* **9**, 323–337.

703 **Finn RD, Clements J, Arndt W, Miller BL, Wheeler TJ, Schreiber F, Bateman A, Eddy**  
704 **SR.** 2015. HMMER web server: 2015 update. *Nucleic acids research* **43**, W30–8.

705 **Foyer CH, Noctor G.** 2005. Redox homeostasis and antioxidant signaling: a metabolic  
706 interface between stress perception and physiological responses. *The Plant cell* **17**, 1866–75.

707 **Fuglsang AT, Kristensen A, Cuin T a., et al.** 2014. Receptor kinase-mediated control of  
708 primary active proton pumping at the plasma membrane. *The Plant Journal* **80**, 951–964.

709 **Gadjev I, Vanderauwera S, Gechev TS, Laloi C, Minkov IN, Shulaev V, Apel K, Inzé D,**  
710 **Mittler R, Van Breusegem F.** 2006. Transcriptomic footprints disclose specificity of  
711 reactive oxygen species signaling in Arabidopsis. *Plant physiology* **141**, 436–45.

712 **García-Mauriño S, Monreal JA, Alvarez R, Vidal J, Echevarría C.** 2003.  
713 Characterization of salt stress-enhanced phosphoenolpyruvate carboxylase kinase activity in  
714 leaves of Sorghum vulgare: independence from osmotic stress, involvement of ion toxicity  
715 and significance of dark phosphorylation. *Planta* **216**, 648–55.

716 **González M-C, Sánchez R, Cejudo FJ.** 2003. Abiotic stresses affecting water balance  
717 induce phosphoenolpyruvate carboxylase expression in roots of wheat seedlings. *Planta* **216**,  
718 985–992.

- 719 **Han SW, Alonso JM, Rojas-Pierce M.** 2015. REGULATOR OF BULB BIOGENESIS1  
720 (RBB1) Is Involved in Vacuole Bulb Formation in Arabidopsis. *PloS one* **10**, e0125621.
- 721 **Harb A, Krishnan A, Ambavaram MMR, Pereira A.** 2010. Molecular and physiological  
722 analysis of drought stress in Arabidopsis reveals early responses leading to acclimation in  
723 plant growth. *Plant physiology* **154**, 1254–71.
- 724 **Haruta M, Burch HL, Nelson RB, Barrett-Wilt G, Kline KG, Mohsin SB, Young JC,**  
725 **Otegui MS, Sussman MR.** 2010. Molecular Characterization of Mutant Arabidopsis Plants  
726 with Reduced Plasma Membrane Proton Pump Activity. *Journal of Biological Chemistry*  
727 **285**, 17918–17929.
- 728 **Hossain MA, Bhattacharjee S, Armin S-M, Qian P, Xin W, Li H-Y, Burritt DJ, Fujita**  
729 **M, Tran L-SP.** 2015. Hydrogen peroxide priming modulates abiotic oxidative stress  
730 tolerance: insights from ROS detoxification and scavenging. *Frontiers in plant science* **6**, 420.
- 731 **Hsieh W-P, Hsieh H-L, Wu S-H.** 2012. Arabidopsis bZIP16 Transcription Factor Integrates  
732 Light and Hormone Signaling Pathways to Regulate Early Seedling Development. *The Plant*  
733 *Cell* **24**, 3997–4011.
- 734 **Hu HC, Wang YY, Tsay YF.** 2009. AtCIPK8, a CBL-interacting protein kinase, regulates  
735 the low-affinity phase of the primary nitrate response. *Plant Journal* **57**, 264–278.
- 736 **Ichimura K, Mizoguchi T, Yoshida R, Yuasa T, Shinozaki K.** 2000. Various abiotic  
737 stresses rapidly activate Arabidopsis MAP kinases ATMPK4 and ATMPK6. *The Plant*  
738 *Journal* **24**, 655–665.
- 739 **Jogaiah S, Govind SR, Tran L-SP.** 2013. Systems biology-based approaches toward  
740 understanding drought tolerance in food crops. *Critical reviews in biotechnology* **33**, 23–39.
- 741 **Kapoor M, Sveenivasan GM.** 1988. The heat shock response of *Neurospora crassa*: Stress-  
742 induced thermotolerance in relation to peroxidase and superoxide dismutase levels.  
743 *Biochemical and Biophysical Research Communications* **156**, 1097–1102.

- 744 **Karpievitch Y V, Dabney AR, Smith RD.** 2012. Normalization and missing value  
745 imputation for label-free LC-MS analysis. *BMC Bioinformatics* **13**, S5.
- 746 **Katam R, Sakata K, Suravajhala P, Pechan T, Kambiranda DM, Naik KS, Guo B,**  
747 **Basha SM.** 2016. Comparative leaf proteomics of drought-tolerant and -susceptible peanut in  
748 response to water stress. *Journal of proteomics* **143**, 209–226.
- 749 **Kline KG, Barrett-Wilt GA, Sussman MR.** 2010. In planta changes in protein  
750 phosphorylation induced by the plant hormone abscisic acid. *Proceedings of the National*  
751 *Academy of Sciences* **107**, 15986–15991.
- 752 **Kohorn BD, Hoon D, Minkoff BB, Sussman MR, Kohorn SL.** 2016. Rapid Oligo-  
753 Galacturonide Induced Changes in Protein Phosphorylation in Arabidopsis. *Molecular &*  
754 *Cellular Proteomics* **15**, 1351–1359.
- 755 **Koopmans F, Cornelisse LN, Heskes T, Dijkstra TMH.** 2014. Empirical bayesian random  
756 censoring threshold model improves detection of differentially abundant proteins. *Journal of*  
757 *Proteome Research* **13**, 3871–3880.
- 758 **Kovtun Y, Chiu WL, Tena G, Sheen J.** 2000. Functional analysis of oxidative stress-  
759 activated mitogen-activated protein kinase cascade in plants. *Proceedings of the National*  
760 *Academy of Sciences of the United States of America* **97**, 2940–5.
- 761 **Krzywińska E, Kulik A, Bucholc M, Fernandez MA, Rodriguez PL, Dobrowolska G.**  
762 2016. Protein phosphatase type 2C PP2CA together with ABI1 inhibits SnRK2.4 activity and  
763 regulates plant responses to salinity. *Plant signaling & behavior* **11**, e1253647.
- 764 **Kulik A, Wawer I, Krzywińska E, Bucholc M, Dobrowolska G.** 2011. SnRK2 Protein  
765 Kinases—Key Regulators of Plant Response to Abiotic Stresses. *OMICS: A Journal of*  
766 *Integrative Biology* **15**, 859–872.
- 767 **Lawlor DW, Tezara W.** 2009. Causes of decreased photosynthetic rate and metabolic  
768 capacity in water-deficient leaf cells: a critical evaluation of mechanisms and integration of

- 769 processes. *Annals of Botany* **103**, 561–579.
- 770 **Lazar C, Gatto L, Ferro M, Bruley C, Burger T.** 2016. Accounting for the Multiple  
771 Natures of Missing Values in Label-Free Quantitative Proteomics Data Sets to Compare  
772 Imputation Strategies. *Journal of Proteome Research* **15**, 1116–1125.
- 773 **Lozano-Sotomayor P, Chávez Montes RA, Silvestre-Vañó M, et al.** 2016. Altered  
774 expression of the bZIP transcription factor DRINK ME affects growth and reproductive  
775 development in *Arabidopsis thaliana*. *The Plant Journal* **88**, 437–451.
- 776 **Marín M, Thallmair V, Ott T.** 2012. The intrinsically disordered N-terminal region of  
777 AtREM1.3 remorin protein mediates protein-protein interactions. *Journal of Biological*  
778 *Chemistry* **287**, 39982–39991.
- 779 **Miller G, Suzuki N, Rizhsky L, Hegie A, Koussevitzky S, Mittler R.** 2007. Double  
780 mutants deficient in cytosolic and thylakoid ascorbate peroxidase reveal a complex mode of  
781 interaction between reactive oxygen species, plant development, and response to abiotic  
782 stresses. *Plant physiology* **144**, 1777–85.
- 783 **Mithoe SC, Ludwig C, Pel MJC, et al.** 2016. Attenuation of pattern recognition receptor  
784 signaling is mediated by a MAP kinase kinase kinase. *EMBO reports* **17**, e201540806.
- 785 **Nakajima M, Shimada A, Takashi Y, et al.** 2006. Identification and characterization of  
786 *Arabidopsis* gibberellin receptors. *Plant Journal* **46**, 880–889.
- 787 **Nemoto K, Ramadan A, Arimura GI, Imai K, Tomii K, Shinozaki K, Sawasaki T.** 2017.  
788 Tyrosine phosphorylation of the GARU E3 ubiquitin ligase promotes gibberellin signalling  
789 by preventing GID1 degradation. *Nature Communications* **8**, 1–7.
- 790 **Nikonorova N, Vu LD, Stes E, Gevaert K, De Smet I.** 2018. Proteome Analysis of  
791 *Arabidopsis* Roots (IN PRESS). *Root Development*.
- 792 **Pandey GK, Kanwar P, Pandey A.** 2014. Functional Role of CBL–CIPK in Abiotic  
793 Stresses. *Global Comparative Analysis of CBL-CIPK Gene Families in Plants*. Cham:



- 794 Springer International Publishing, 65–77.
- 795 **Passaia G, Spagnolo Fonini L, Caverzan A, Jardim-Messeder D, Christoff AP, Gaeta**  
796 **ML, de Araujo Mariath JE, Margis R, Margis-Pinheiro M.** 2013. The mitochondrial  
797 glutathione peroxidase GPX3 is essential for H<sub>2</sub>O<sub>2</sub> homeostasis and root and shoot  
798 development in rice. *Plant Science* **208**, 93–101.
- 799 **Pereyra-Irujo GA, Velázquez L, Lechner L, Aguirrezábal LAN.** 2008. Genetic variability  
800 for leaf growth rate and duration under water deficit in sunflower: analysis of responses at  
801 cell, organ, and plant level. *Journal of experimental botany* **59**, 2221–32.
- 802 **Pitzschke A, Hirt H.** 2006. Mitogen-activated protein kinases and reactive oxygen species  
803 signaling in plants. *Plant physiology* **141**, 351–6.
- 804 **Pitzschke A, Schikora A, Hirt H.** 2009. MAPK cascade signalling networks in plant  
805 defence. *Current Opinion in Plant Biology* **12**, 421–426.
- 806 **Qin N, Xu W, Hu L, Li Y, Wang H, Qi X, Fang Y, Hua X.** 2016. Erratum to: Drought  
807 tolerance and proteomics studies of transgenic wheat containing the maize C4  
808 phosphoenolpyruvate carboxylase (PEPC) gene. *Protoplasma* **253**, 1513–1513.
- 809 **Ramachandra Reddy A, Chaitanya KV, Vivekanandan M.** 2004. Drought-induced  
810 responses of photosynthesis and antioxidant metabolism in higher plants. *Journal of plant*  
811 *physiology* **161**, 1189–202.
- 812 **Rasheed S, Bashir K, Matsui A, Tanaka M, Seki M.** 2016. Transcriptomic Analysis of  
813 Soil-Grown *Arabidopsis thaliana* Roots and Shoots in Response to a Drought Stress.  
814 *Frontiers in plant science* **7**, 180.
- 815 **Rieu I, Eriksson S, Powers SJ, et al.** 2008. Genetic analysis reveals that C19-GA 2-  
816 oxidation is a major gibberellin inactivation pathway in *Arabidopsis*. *The Plant cell* **20**, 2420–  
817 36.
- 818 **Rudashevskaya EL, Ye J, Jensen ON, Fuglsang AT, Palmgren MG.** 2012. Phosphosite

819 mapping of P-type plasma membrane H<sup>+</sup>-ATPase in homologous and heterologous  
820 environments. *The Journal of biological chemistry* **287**, 4904–13.

821 **Sánchez R, Flores A, Cejudo FJ.** 2006. Arabidopsis phosphoenolpyruvate carboxylase  
822 genes encode immunologically unrelated polypeptides and are differentially expressed in  
823 response to drought and salt stress. *Planta* **223**, 901–909.

824 **Schindelin J, Rueden CT, Hiner MC, Eliceiri KW.** 2015. The ImageJ ecosystem: An open  
825 platform for biomedical image analysis. *Molecular Reproduction and Development* **82**, 518–  
826 529.

827 **Shavrukov Y.** 2013. Salt stress or salt shock: which genes are we studying? *Journal of*  
828 *Experimental Botany* **64**, 119–127.

829 **Shi H, Yan H, Li J, Tang D.** 2013. BSK1, a receptor-like cytoplasmic kinase, involved in  
830 both BR signaling and innate immunity in Arabidopsis. *Plant Signaling & Behavior* **8**,  
831 e24996.

832 **Singh R, Jwa N-S.** 2013. Understanding the responses of rice to environmental stress using  
833 proteomics. *Journal of proteome research* **12**, 4652–69.

834 **Skirycz A, Claeys H, De Bodt S, et al.** 2011a. Pause-and-stop: the effects of osmotic stress  
835 on cell proliferation during early leaf development in Arabidopsis and a role for ethylene  
836 signaling in cell cycle arrest. *The Plant cell* **23**, 1876–88.

837 **Skirycz A, Memmi S, De Bodt S, Maleux K, Obata T, Fernie AR, Devreese B, Inzé D.**  
838 2011b. A reciprocal <sup>15</sup>N-labeling proteomic analysis of expanding Arabidopsis leaves  
839 subjected to osmotic stress indicates importance of mitochondria in preserving plastid  
840 functions. *Journal of Proteome Research* **10**, 1018–1029.

841 **Skirycz A, Vandenbroucke K, Clauw P, et al.** 2011c. Survival and growth of Arabidopsis  
842 plants given limited water are not equal. *Nature biotechnology* **29**, 212–4.

843 **Stecker KE, Minkoff BB, Sussman MR.** 2014. Phosphoproteomic Analyses Reveal Early

- 844 Signaling Events in the Osmotic Stress Response. *Plant Physiology* **165**, 1171–1187.
- 845 **Tarrant MK, Cole PA.** 2009. The Chemical Biology of Protein Phosphorylation. Annual  
846 Review of Biochemistry **78**, 797–825.
- 847 **Ueguchi-Tanaka M, Ashikari M, Nakajima M, et al.** 2005. GIBBERELLIN  
848 INSENSITIVE DWARF1 encodes a soluble receptor for gibberellin. *Nature* **437**, 693–698.
- 849 **Vanderauwera S, Zimmermann P, Rombauts S, Vandenabeele S, Langebartels C,**  
850 **Gruissem W, Inzé D, Van Breusegem F.** 2005. Genome-wide analysis of hydrogen  
851 peroxide-regulated gene expression in Arabidopsis reveals a high light-induced  
852 transcriptional cluster involved in anthocyanin biosynthesis. *Plant physiology* **139**, 806–21.
- 853 **Verslues PE.** 2017. Time to grow: factors that control plant growth during mild to moderate  
854 drought stress. *Plant, cell & environment* **40**, 177–179.
- 855 **Verslues PE, Agarwal M, Katiyar-Agarwal S, Zhu J, Zhu J-K.** 2006a. Methods and  
856 concepts in quantifying resistance to drought, salt and freezing, abiotic stresses that affect  
857 plant water status. *The Plant journal* □: for cell and molecular biology **45**, 523–39.
- 858 **Verslues PE, Guo Y, Dong C-H, Ma W, Zhu J-K.** 2006b. Mutation of SAD2, an importin  
859 beta-domain protein in Arabidopsis, alters abscisic acid sensitivity. *The Plant journal* □: for  
860 cell and molecular biology **47**, 776–87.
- 861 **Vu LD, Stes E, Van Bel M, Nelissen H, Maddelein D, Inzé D, Coppens F, Martens L,**  
862 **Gevaert K, De Smet I.** 2016. Up-to-Date Workflow for Plant (Phospho)proteomics  
863 Identifies Differential Drought-Responsive Phosphorylation Events in Maize Leaves. *Journal*  
864 *of Proteome Research* **15**, 4304–4317.
- 865 **Walley JW, Sartor RC, Shen Z, et al.** 2016. Integration of omic networks in a  
866 developmental atlas of maize. *Science (New York, N.Y.)* **353**, 814–8.
- 867 **Wang F, Chen Z-H, Shabala S.** 2017a. Hypoxia Sensing in Plants: On a Quest for Ion  
868 Channels as Putative Oxygen Sensors. *Plant and Cell Physiology* **58**, 1126–1142.

- 869 **Wang H, Chevalier D, Larue C, Ki Cho S, Walker JC.** 2007. The Protein Phosphatases  
870 and Protein Kinases of *Arabidopsis thaliana*. The *Arabidopsis Book* **5**, e0106.
- 871 **Wang J, Li L, Chen T, Ma J, Zhu Y, Zhuang J, Chang C.** 2017*b*. In-depth method  
872 assessments of differentially expressed protein detection for shotgun proteomics data with  
873 missing values. *Scientific Reports* **7**, 3367.
- 874 **Wang W, Vinocur B, Altman A.** 2003. Plant responses to drought, salinity and extreme  
875 temperatures: towards genetic engineering for stress tolerance. *Planta* **218**, 1–14.
- 876 **Wang W, Ye R, Xin Y, Fang X, Li C, Shi H, Zhou X, Qi Y.** 2011. An importin  $\beta$  protein  
877 negatively regulates MicroRNA activity in *Arabidopsis*. *The Plant cell* **23**, 3565–76.
- 878 **van Wijk KJ, Friso G, Walther D, Schulze WX.** 2014. Meta-Analysis of *Arabidopsis*  
879 *thaliana* Phospho-Proteomics Data Reveals Compartmentalization of Phosphorylation Motifs.  
880 *The Plant Cell* **26**, 2367–2389.
- 881 **Xue L, Wang P, Wang L, Renzi E, Radivojac P, Tang H, Arnold R, Zhu J-K, Tao WA.**  
882 2013. Quantitative measurement of phosphoproteome response to osmotic stress in  
883 *Arabidopsis* based on Library-Assisted eXtracted Ion Chromatogram (LAXIC). *Molecular*  
884 *and Cellular Proteomics* **53**, 1–39.
- 885

## 886 TABLES

887 **Table 1.** Phosphorylated sites mentioned in text.

Group	Protein	Name (TAIR)	Position	Log2 fold change	Localisation probability	Peptide with localisation probabilities
Upregulated	AT3G19100	CALCIUM-DEPENDENT PROTEIN KINASE (CDPK/CPK)-RELATED PROTEIN KINASE 2 (TAGK2/CRK2)	Ser <sup>57</sup>	0.683	0.95	ASPFPPFY(0.02)T(0.03)PS(0.95)PAR
	AT2G21230	BASIC LEUCINE-ZIPPER 30 (BZIP30)	Ser <sup>176</sup>	0.665	1.00	SIS(1)GEDTSDWSNLVK
	AT3G13290	VARICOSE-RELATED PROTEIN (VCR)	Ser <sup>680</sup>	0.552	0.99	T(0.005)S(0.005)S(0.99)ADY(0.001)FYVR
	AT1G28280	MPK3/6-TARGETED VQ MOTIF-CONTAINING PROTEIN 1 (MVQ1)	Ser <sup>194</sup>	0.618	0.95	S(0.018)GS(0.018)S(0.018)NQS(0.945)PNELAAEEK
Downregulated	AT3G13530	MITOGEN-ACTIVATED PROTEIN KINASE KINASE KINASE 7 (MAPKKK7)	Ser <sup>776</sup>	-0.274	0.95	LAS(0.051)IS(0.95)GGLDGQAPR
	AT2G45820	REMORIN 1.3 (REM1.3)	Thr <sup>58</sup>	-0.460	1.00	ALAVVEKPIEHT(1)PK
			Ser <sup>64</sup>	-0.450	0.95	AS(0.01)S(0.95)GS(0.04)ADRDVILADLEK
	AT2G35530	BASIC REGION/LEUCINE ZIPPER TRANSCRIPTION FACTOR 16 (bZIP16)	Ser <sup>152</sup>	-0.708	1.00	GS(1)LGSLNMITGK
Unique for manitol	AT4G24400	CBL-INTERACTING PROTEIN KINASE 8 (CIPK8); SNF1-RELATED PROTEIN KINASE 3.13 (SnRK3.13)	Thr <sup>166</sup>	-	0.85	T(0.85)T(0.15)CGTPNYVAPEVLSHK
Unique for control	AT5G40450	REGULATOR OF BULB BIOGENESIS (RBB1)	Ser <sup>2802</sup>	-	1.00	S(0.997)LS(0.003)DHIQK
	AT4G35230	BRASSINOSTEROID-SIGNALING KINASE 1 (BSK1)	Thr <sup>353</sup>	-	0.80	KQEEAPS(0.201)T(0.798)PQRPLS(0.001)PLGEACSR
	AT1G10940	SNF1-RELATED PROTEIN KINASE 2.4 (SNRK2.4)	Ser <sup>357</sup>	-	1.00	EVHAS(1)GEVR

888 **Table 2.** Details on phosphoproteomic studies for comparative analysis

Study	Material	Growth medium	Compound	Concentration	Time	Setup	Method
Current study	Leaf #3 of 15-days-old seedlings	Agar plates	Mannitol	25 mM	30 min	Transfer	Label-free
Bhaskara et al., 2017	7-day-old seedlings	Agar plates	PEG	a low water potential (21.2 MPa)	96 h	Transfer	ITRAQ
Stecker et al., 2014	10-day-old seedlings	Liquid culture	Mannitol	300mM	5 min	Medium replacement	<sup>15</sup> N-labelling
Xue et al., 2013	12-day-old seedlings	Liquid culture	Mannitol	800mM	30 min	Transfer	Label-free

889

890

891

892

893

894

895

896

897

898

899 **FIGURE LEGENDS**

900

901 **Figure 1. Mannitol-triggered protein and phosphoprotein changes upon short exposure**  
902 **(30 min).** This workflow illustrates the steps to obtain a reliable set of proteins or  
903 phosphosites following LC-MS/MS. The portions for proteins and phosphosites (including  
904 the % serine (S), threonine (T) and tyrosine (Y) sites) are indicated.

905

906 **Figure 2. Mannitol-triggered protein changes upon long exposure (4 h).** This workflow  
907 illustrates the steps to obtain a reliable set of proteins following LC-MS/MS. The numbers for  
908 detected and selected proteins are indicated.

909

910 **Figure 3.** Protein-protein interaction network of significant mannitol-regulated proteins (30  
911 min treatment). GO annotations for biological process of up- and down-regulated proteins  
912 were superimposed on the network and nodes were grouped accordingly. Colored  
913 backgrounds indicate functions related to protein metabolism (yellow), photosynthesis and  
914 carbohydrate metabolism (green) and oxidation-reduction processes (orange). Unique  
915 proteins were indicated with dashed lines while differentially abundant proteins were  
916 coloured from dark green ranging to red depending on the  $\log_2$  fold change. Thickness of  
917 connecting lines indicates a combined score of interaction.

918

919 **Figure 4.** Comparison of protein abundance with transcript level of corresponding genes. The  
920 differential expression of significant differentially up- or down-regulated proteins was  
921 analysed. The expression and protein levels were measured in expanding leaf tissue upon  
922 mannitol treatment and compared to control conditions. Dashed lines indicate proteins unique  
923 for control (green) or mannitol-treated (red) samples. RAD23C - RADIATION

924 SENSITIVE23C; 4CL1 - 4-COUMARATE:COA LIGASE 1; PRXQ - PEROXIREDOXIN  
925 Q; CDSP32 - CHLOROPLASTIC DROUGHT-INDUCED STRESS PROTEIN OF 32 KD;  
926 LEA26 - LATE EMBRYOGENESIS ABUNDANT 26; SAL1 – SAL1 phosphatase;  
927 EIF(ISO)4E - EUKARYOTIC TRANSLATION INITIATION FACTOR ISOFORM 4E;  
928 FAD7 - FATTY ACID DESATURASE 7; CAT1 – CATALASE 1.

929

930 **Figure 5.** Protein-protein interaction network of significant mannitol-regulated proteins (4 h  
931 treatment). GO annotations for biological process of up- and down-regulated proteins were  
932 superimposed on the network and nodes were grouped accordingly. Unique proteins were  
933 indicated with dashed lines while differentially abundant proteins were coloured from dark  
934 green ranging to red depending on the  $\log_2$  fold change. Thickness of connecting lines  
935 indicates a combined score of interaction.

936

937 **Figure 6.** Venn diagram showing the overlap between the significant up- and down-regulated  
938 proteins from the 30 min proteome data set and all quantifiable proteins from 4 h proteome  
939 data set. In the overlap, three subsets of proteins are identified based on the changes in their  
940 abundances from 30 min to 4 h of mannitol stress; stable proteins are up- or downregulated at  
941 both 30 min and 4 h, “UP to DOWN” indicate proteins that are upregulated after 30 min but  
942 downregulated at 4 h and the “DOWN to UP” indicates the opposite.

943

944 **Figure 7.** Protein-protein interaction network of significant mannitol-regulated  
945 phosphopeptides mapped on the corresponding proteins (30 min treatment). GO annotations  
946 for biological process of up- and down-regulated proteins were superimposed on the network  
947 and nodes were grouped accordingly. Unique phosphosites were indicated with dashed lines  
948 while differentially abundant phosphosites were coloured from dark green ranging to red



949 depending on the  $\log_2$  fold change. Thickness of connecting lines indicates a combined score  
950 of interaction.

951

952 **Figure 8.** A normalised mannitol-triggered phosphoproteome. Significantly up- and  
953 downregulated phosphosites were normalised by subtracting the  $\log_2$  fold change of the  
954 protein abundance from the  $\log_2$  fold change of the phosphosite, with the exception of the  
955 unique phosphosites. In total, 32 differentially phosphorylated proteins could be mapped on  
956 total proteome data. RBB1- REGULATOR OF BULB BIOGENESIS1; PHOS34 -  
957 Phosphorylated protein of 34 kDa; NDK1 - NUCLEOSIDE DIPHOSPHATE KINASE 1;  
958 ADSS - ADENYLOSUCCINATE SYNTHASE; CPN20 - CHAPERONIN 20; REM1.3 -  
959 Remorin 1.3; PSAE1 - Photosystem I reaction center subunit IV A; H1.2 - HISTONE 1.2;  
960 REC2 - REDUCED CHLOROPLAST COVERAGE 2; PHOT1 - PHOTOTROPIN 1; TOC86  
961 - TRANSLOCON AT THE OUTER ENVELOPE MEMBRANE OF CHLOROPLASTS 86;  
962 AMPD - ADENOSINE 5'-MONOPHOSPHATE DEAMINASE; ELF5A-3 - EUKARYOTIC  
963 ELONGATION FACTOR 5A-3; AHA2 - H(+)-ATPASE 2; PSBA - PHOTOSYSTEM II  
964 REACTION CENTER PROTEIN A; REC3 - REDUCED CHLOROPLAST COVERAGE 3;  
965 PIP3 - PLASMA MEMBRANE INTRINSIC PROTEIN 3; RBCS1A - RIBULOSE  
966 BISPHOSPHATE CARBOXYLASE SMALL CHAIN 1A; DAYSLEEPER - Zinc finger  
967 BED domain-containing protein; CRWN1 - CROWDED NUCLEI 1.

968

969 **Figure 9.** Venn diagram showing the overlapping phosphoproteins from four recent  
970 phosphoproteomic studies of osmotic stress responses, including our current study. Details on  
971 selected studies, concerning the osmoticum and concentration that was used, are indicated in  
972 Table 2. bZIP30 - BASIC LEUCINE-ZIPPER 30; RBB1- REGULATOR OF BULB

973 BIOGENESIS1; VCR - VARICOSE-RELATED PROTEIN; MVQ1 - MPK3/6-TARGETED  
974 VQ MOTIF-CONTAINING PROTEIN 1.

975

976 **Figure 10. Phenotypes of T-DNA insertion lines for selected candidates. (A, C)**  
977 Representative pictures of *crrsp38-1* and *aha2-4* lines compared to Col-0 at 22 days after  
978 stratification grown on control (MS) or mannitol (25 mM). Scale bar, 5 mm. **(B, D)**  
979 Quantification of the rosette area of *crrsp38-1* (B) and *aha2-4* (D) at 22 days after  
980 stratification grown on control (MS) or 25 mM mannitol (MA). Boxplots are combined  
981 values of at least 30 seedlings from 4-6 different plates and 2 or 1 independent experiments  
982 for *crrsp38-1* or *aha2-4*, respectively. Asterisk indicates a significant difference with  $p < 0.05$   
983 based on ANOVA. In addition, the ANOVA analysis indicated that the genotype:treatment  
984 interaction for *aha2-4* was significant ( $p < 0.05$ ).

# PROTEOME

LC-MS/MS  
Protein identification (MaxQuant)

2991 proteins

Only identified by site,  
Contaminants, Reverse

2932 proteins

Log2 transformation of intensities

Missing values  
(75% of replicates are valid  
in at least one sample)



18  
1911  
21

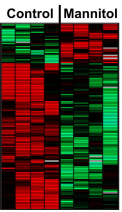
Missing values  
(75% of replicates are valid  
in both samples)

1823 proteins

Centering (subtraction)  
Two sample t-test ( $p \leq 0.05$ )

128 proteins

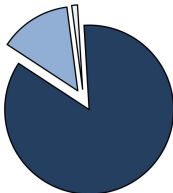
Z-scoring



-2.25 0 2.00

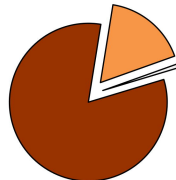
Missed  
cleavages

■ 0 ■ 1 □ 2



Phosphorylation  
site

■ pS ■ pT □ pY



# PHOSPHOPROTEOME

LC-MS/MS  
Protein identification (MaxQuant)

3747 phosphosites

Contaminants, Reverse



3698 phosphosites

Log2 transformation of intensities

Missing values  
(75% of replicates are valid  
in at least one sample)



56  
1622  
40

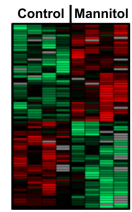
Missing values  
(75% of replicates are valid  
in both samples)

1332 phosphosites

Centering (subtraction)  
Two sample t-test ( $p \leq 0.05$ )

76 phosphosites

Z-scoring



-2.0 0 2.0

✓ Network  
analysis  
✓ GO annotation  
✓ Functional  
validation

27 proteins are  
UPREGULATED

101 proteins are  
DOWNREGULATED

56 phosphosites  
(= 55 proteins)  
are UNIQUE  
for control

40 phosphosites  
(= 38 proteins)  
are UNIQUE  
for mannitol

40 phosphosites  
(= 37 proteins)  
are  
UPREGULATED

36 phosphosites  
(= 34 proteins)  
are  
DOWNREGULATED

FIGURE 1

# PROTEOME

LC-MS/MS  
Protein identification (MaxQuant)

2675 proteins

Only identified by site,  
Contaminants, Reverse

2633 proteins

Transformation (Log2)

Missing values  
(75% of replicates are valid  
in at least one sample)



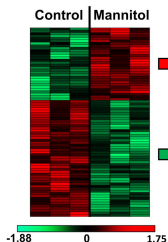
Missing values  
(75% of replicates are valid  
in both samples)

1544 proteins

Centering (subtraction)  
Two sample t-test ( $p \leq 0.05$ )

78 proteins

Z-scoring



14 proteins  
are **UNIQUE**  
for control

1 protein  
is **UNIQUE**  
for mannitol

✓ Protein  
interaction  
analysis  
(*in silico*)

✓ GO annotation

30 proteins  
are  
**UPREGULATED**

48 proteins  
are  
**DOWNREGULATED**

Missed  
cleavages

0 1 2



FIGURE 2

### Translation and ribosome biogenesis

### Folding

### Protein catabolism

### Protein transport

### Amino acid biosynthesis

### Cytoskeleton organisation

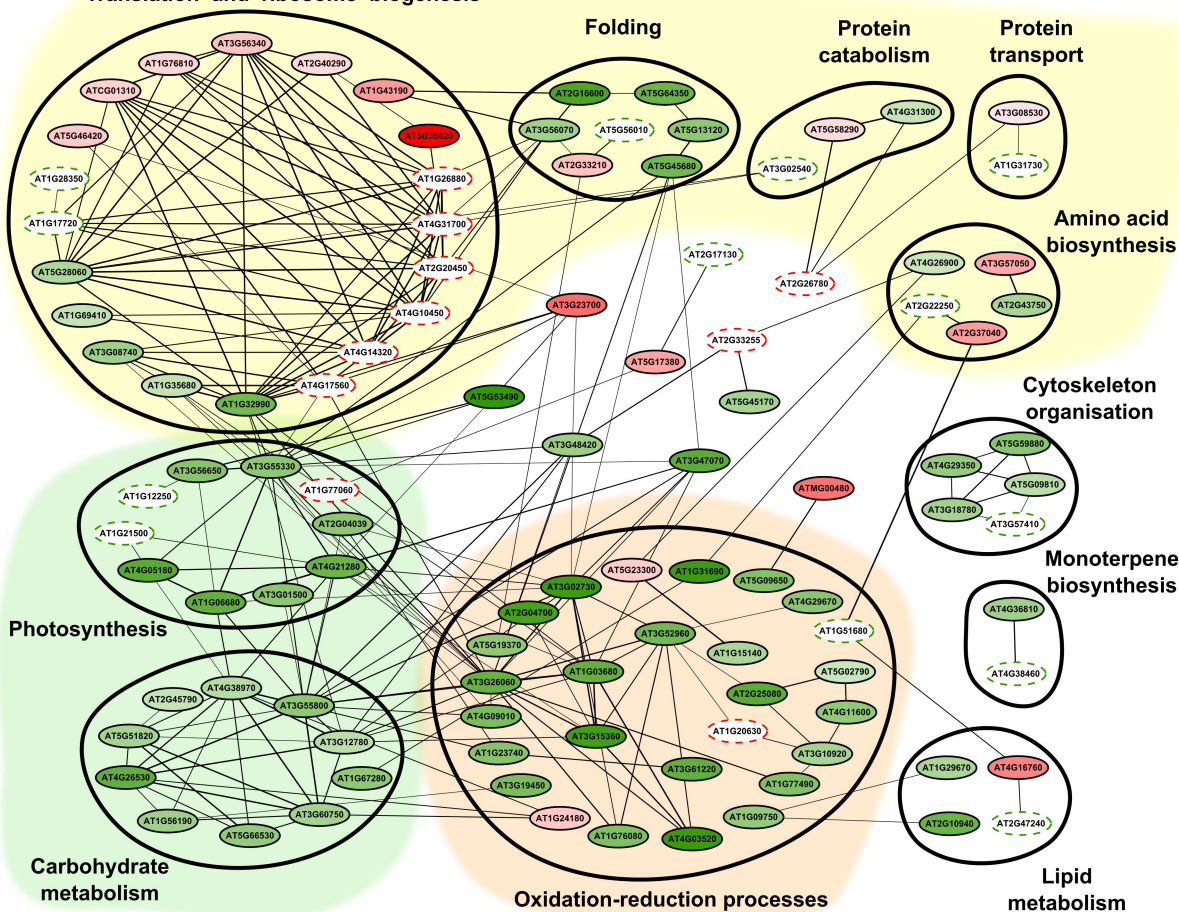
### Monoterpene biosynthesis

### Lipid metabolism

### Oxidation-reduction processes

### Photosynthesis

### Carbohydrate metabolism



Unique for control



Log2 fold change



Unique for mannitol



FIGURE 3

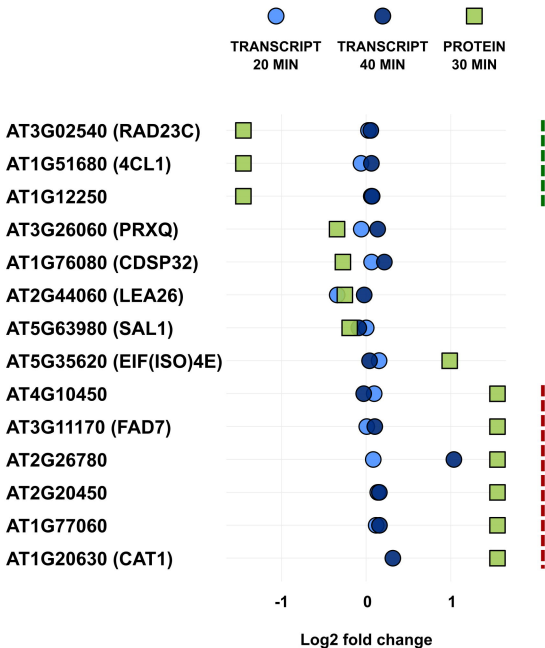
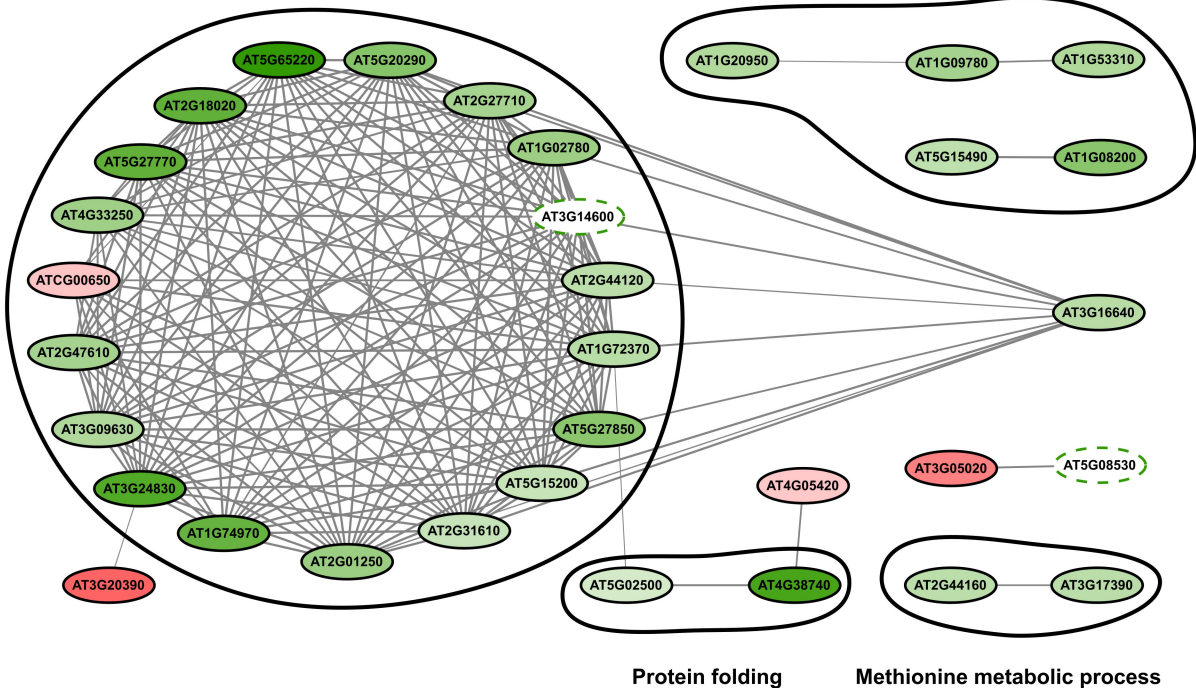


**FIGURE 4**

Translation and ribosome biogenesis

Photosynthesis and carbohydrate metabolism



Unique for control

Log2 fold change



-0.71

0.0

1.17

FIGURE 5

**30 min proteome  
(up- and downregulated  
proteins)**

**4 h proteome  
(all quantifiable  
proteins)**

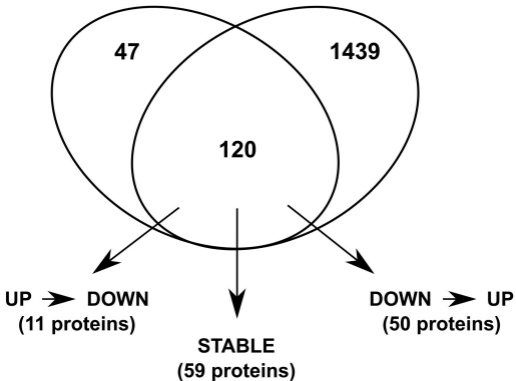


**FIGURE 6**



Photosynthesis and chloroplast relocation

Cuticle development

Chromatin remodeling

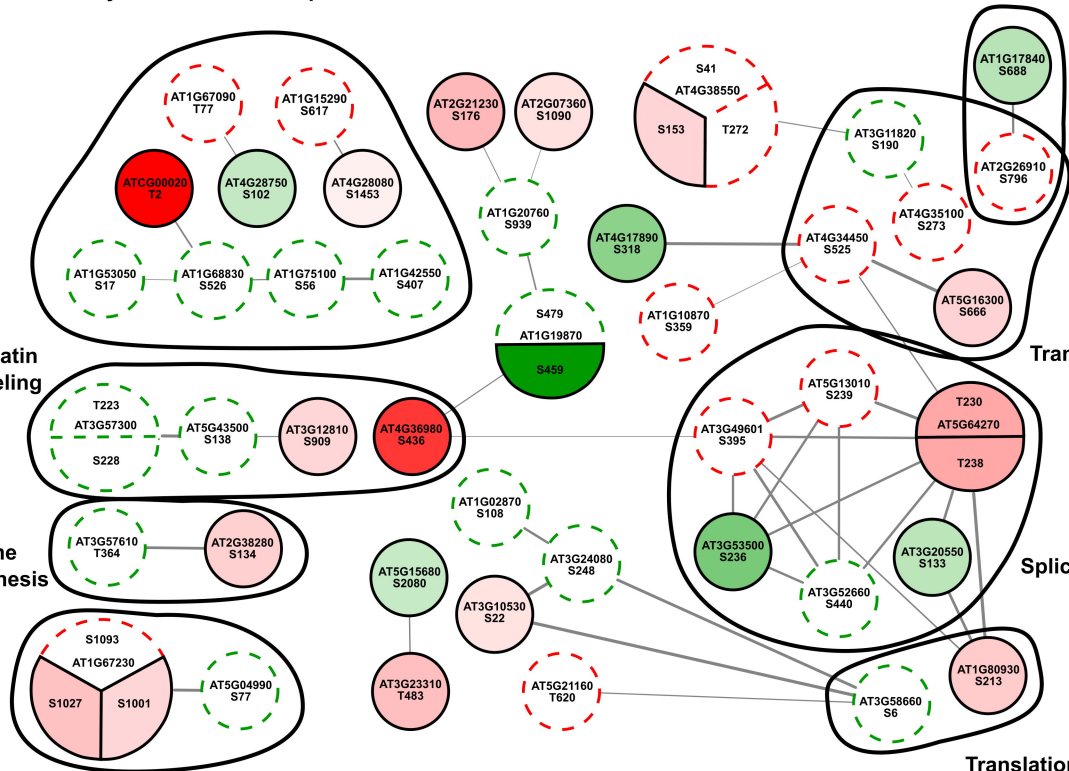
Purine biosynthesis

Nucleus organisation

Transport

Splicing

Translation



Unique for control



Log2 fold change



-0.7

0.0

2.4

Unique for mannitol



FIGURE 7

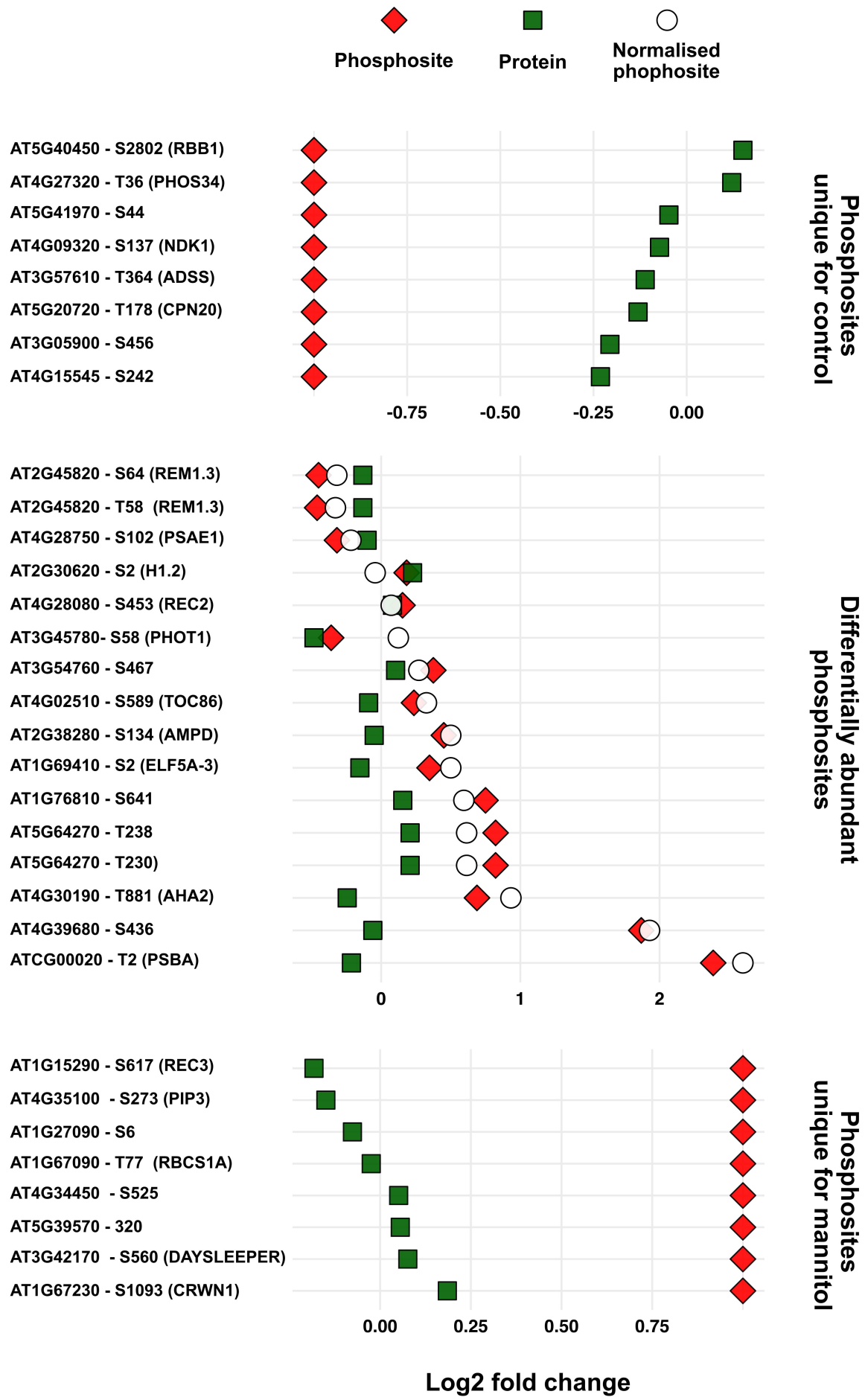


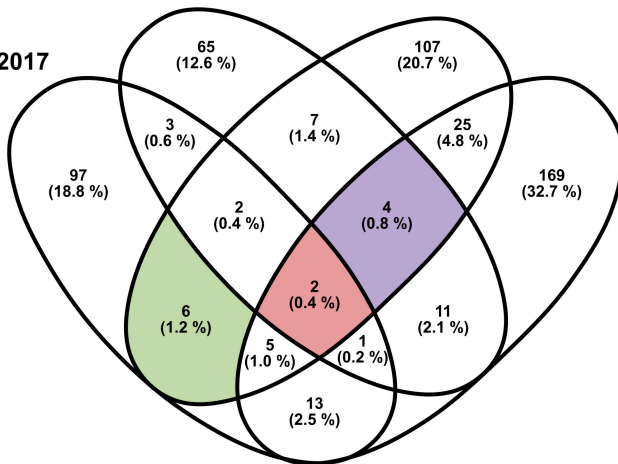
FIGURE 8

Stecker et al., 2014


Current study

Bhaskara et al., 2017

Xue et al., 2013



 Osmotic stress  
(bZIP30, RBB1)

 Mannitol stress  
(e.g. VCR)


 Mild osmotic stress  
(e.g. MVQ1)

FIGURE 9

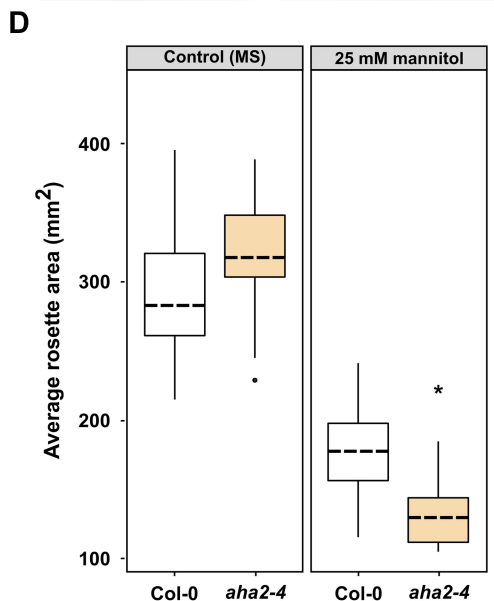
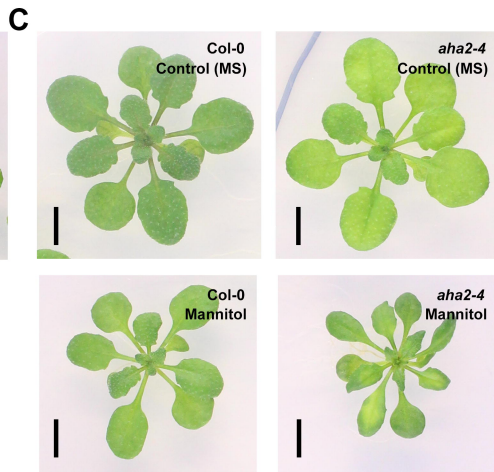
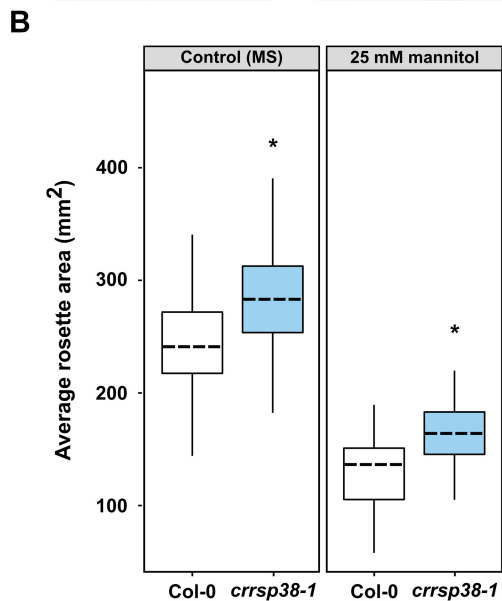
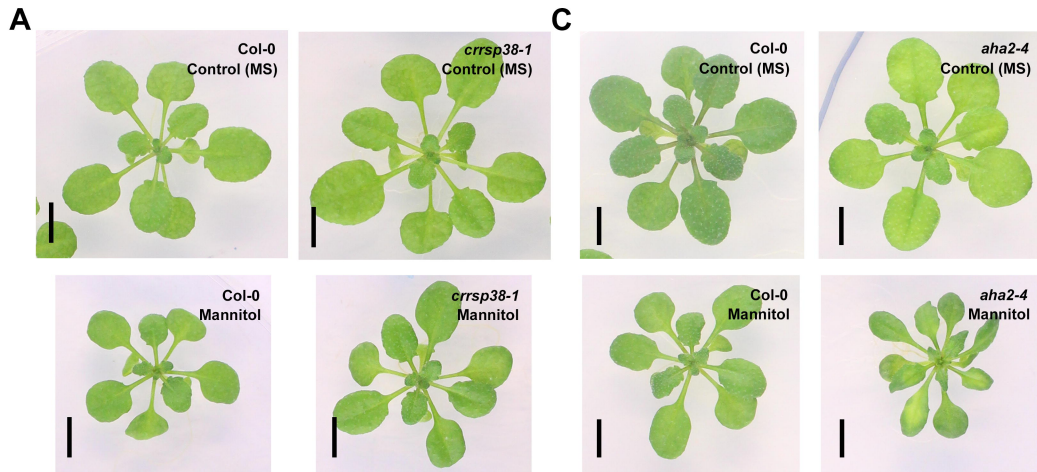


FIGURE 10